



Institut für Physikalische Elektronik

Institute of Physical Electronics

Universität Stuttgart

Jahresbericht

Annual Report

2003

Institut für Physikalische Elektronik
Pfaffenwaldring 47
D-70569 Stuttgart
Tel.: +49-711-685-7141
Fax: +49-711-685-7143
<http://www.ipe.uni-stuttgart.de>

Redaktion/edited by:
Hans-Werner Schock
Uwe Rau
Fritz Pfisterer
Jürgen H. Werner

Inhaltsverzeichnis / Table of Contents

1	Vorwort / Preface	4
2	Lehre am ipe / Teaching at the ipe	6
2.1	Vorlesung <i>Bauelemente der Mikroelektronik I</i>	6
2.2	Vorlesung <i>Festkörperelektronik I</i>	6
2.3	Vorlesung <i>Optoelectronic Devices and Circuits I (Optoelektronik II)</i>	7
2.4	Vorlesung <i>Photovoltaics</i>	8
2.5	Vorlesung <i>Energiewandlung</i>	8
2.6	Vorlesung <i>Lasers and Light Sources</i>	10
2.7	Vorlesung <i>Thin Film Characterization Methods</i>	10
2.8	Praktika	11
3	Menschen am ipe / People at the ipe	12
3.1	Verwaltung, Werkstatt und Institutsleitung / <i>Administration, Workshop, and Head of Institute</i>	13
3.2	Gruppe Silicium / <i>Group Silicon</i>	14
3.3	Gruppe Verbindungshalbleiterschichten / <i>Group Compound Semiconductor Films</i>	16
3.4	Gruppe Laserprozesse / <i>Group Laser Processing</i>	18
3.5	Gruppe CIS Technologie und Oberflächenanalyse / <i>Group CIS Technology and Surface Analysis</i>	20
3.6	Gruppe Bauelementanalyse / <i>Group Device Analysis</i>	22

4	Wissenschaftliche Beiträge / Scientific Contributions	24
	U. RAU: <i>Role of the Cu(In, Ga)Se₂ Surface Defect Layer</i>	24
	J.H. WERNER: <i>Efficiency Limitations of Cu(In, Ga)Se₂ Solar Cells</i>	26
	T. SCHLENKER: <i>Grain Growth in Thin Cu(In, Ga)Se₂ Films</i>	28
	G. HANNA: <i>Film Texture and Grain Boundary Activity in Cu(In, Ga)Se₂ Films</i>	30
	K. ORGASSA: <i>Optical Constants of Cu(In, Ga)Se₂ Thin Films</i>	32
	G. C. GLÄSER: <i>Analysis of Granular CuInSe₂ by Electron Beam Induced Current</i>	34
	P.O. GRABITZ: <i>Mechanical Properties of Flexible Cu(In, Ga)Se₂ Solar Cells</i>	36
	G. BILGER: <i>Cu(In, Ga)Se₂ Layers Analyzed by Corrected SIMS Depth Profiles</i>	38
	A. ESTURO-BRETON: <i>Laser-Doping of n+-type Silicon Solar Cell Emitters</i>	40
	C. BERGE: <i>Monocrystalline Transfer Silicon with 150 mm Diameter</i>	42
	M. SCHUBERT: <i>Recent Developments in Integrated Photovoltaics</i>	44
	K. TARETTO: <i>Expression for the Current/Voltage Characteristics of pin Solar Cells</i> ..	46
	G. KRON: <i>The Built-in Voltage and the Fill Factor of Dye Sensitized Solar Cells</i>	48
5	Verzeichnis der Publikationen / List of Publications	50
6	Promotionen 2003 / Ph.D. Theses 2003	53
7	Diplomarbeiten 2003 / Diploma Thesis Projects 2003	54
8	Studienarbeiten 2003 / Major Term Projects 2003	55
9	ipe Kolloquium 2003	56
10	Gäste und ausländische Stipendiaten / Guests	57
11	Wissenschaftliche Geräte und Analysemethoden	59
	<i>/ Scientific Instruments and Methods of Analysis</i>	
	11.1 Abscheideverfahren / <i>Deposition Methods</i>	59
	11.2 Strukturelle Analyseverfahren / <i>Structural Materials Analysis</i>	60
	11.3 Analyse optischer Eigenschaften / <i>Analysis of Optical Properties</i>	61
	11.4 Analyse elektro-optischer Eigenschaften / <i>Electro-optical Properties</i>	62
12	Mitarbeiterliste / Staff Members	63
13	Lageplan / Site Plan	66

1 Vorwort

Liebe Freunde des *ipe*,

Sie halten hier den Siebten der Jahresberichte des *ipe* in Händen; wir informieren Sie über unsere Arbeit im Jahr 2003. Wer die Berichte in den letzten Jahren aufmerksam verfolgt hat, wird bemerkt haben, dass wir uns immer mehr auf unser Kerngeschäft konzentriert haben: *Physik und Technologie der Halbleitermaterialien und -bauelemente*. Nur so können wir unseren Standard in der immer härteren Konkurrenz um erstklassiges Personal und um Forschungsgelder halten.

Die Stärke des *ipe* ist es, Grundlagenforschung mit der Anwendung bis hin zur direkten Kooperation mit der Industrie zu verbinden. Unser Drittmittelumsatz von über 2,5 Millionen Euro mit 20% direktem Industrieanteil spricht für sich. Über 35 der derzeit 47 Mitarbeiter/innen (ohne Studenten, ohne Gäste) des *ipe* werden aus diesen Drittmitteln bezahlt. Dennoch haben im Jahr 2003 am *ipe* wieder 8 junge Wissenschaftler in einer Zeit von etwa 3 ½ Jahren promoviert.

Im Jahr 2003 haben sich zehn deutsche Universitätsinstitute, die auf dem Gebiet der Photovoltaik forschen, zum Forschungsverbund *PV-Uni-Netz* zusammen geschlossen. Ziel des Verbundes ist es, die Forschung besser zu koordinieren und nach außen hin besser darzustellen. Zur Zeit fungiere ich selbst als Sprecher dieses Verbundes. Wir werden sehen, ob dieser Zusammenschluss zu einer Stärkung der Photovoltaik-Forschung an deutschen Universitäten führen wird.

Ich bedanke mich an dieser Stelle ganz herzlich bei allen Mitarbeitern des *ipe*, meinen Kollegen in der Fakultät, meinen Freunden sowie der Leitung und Verwaltung der Universität Stuttgart für die Unterstützung meiner Forschung und Lehre der letzten 7 ½ Jahre.

Stuttgart, Dezember 2003



Jürgen H. Werner

1 Preface

Dear friends of the *ipe*,

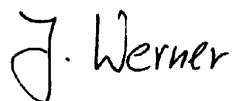
You are holding in your hands the seventh Annual Report of the *ipe*; we are informing you about our work during the year 2003. Those who have followed our annual reports in the last years will notice that we concentrate more and more on our main expertise: *Physics and Technology of Semiconductor Materials and Devices*. This is the only way to maintain our high standard in the increasingly harder competition for first class staff and for research funds.

The strength of the *ipe* lies in combining basic research with applications and direct cooperation with industry. Our annual turnover of more than 2.5 million Euros with a 20% share of direct industry funding speaks for itself. More than 35 persons of our staff at present (a total of 47 persons, students and guests not included) are being paid from research funds. Nevertheless, in 2003 again 8 young scientists completed their PhD-thesis within about 3 ½ years.

In the year 2003, ten German university institutes engaged in photovoltaics research formed the research network *PV-Uni-Netz*. This network aims at improved research coordination and at a better presentation of research results to the public. At present, I have the honour of being the speaker of this association. We shall see whether this joining together yields a reinforcement of the photovoltaics research at German Universities.

At this place, I would like to express my sincere thanks to the whole *ipe* staff, to my colleagues of the Faculty, to my friends and to the rector and administration of the Stuttgart University for the support given to my research and teaching work during the last 7 ½ years.

Stuttgart, December 2003



Jürgen H. Werner

2 Lehre am ipe / Teaching at the ipe

2.1 Vorlesung Bauelemente der Mikroelektronik

Einführung: Diverse Informationen; Geschichte der Halbleiterbauelemente; Mikroelektronik heute.

Leitfähigkeit und Energiebänder: Spezifischer Widerstand; Energiebänder.

Silicium – der Werkstoff der Mikroelektronik: Periodensystem der Elemente; Element Si; Siliciumkristalle; Herstellung von hochreinen Siliciumscheiben; Siliciumdioxid als Schutzschicht für Silicium; Herstellung einer integrierten Schaltung durch Planarprozess; kleinere Strukturen und größere Scheiben (Wafer); Dotieren von Silicium.

Elektronen und Löcher in Halbleitern: Das Loch als Quasiteilchen; Ladung des Loches; Energie von Elektronen und Löchern; effektive Masse m^* ,

elektrisches Feld \mathcal{E} und Potential φ .

Ströme in Halbleitern: Leitfähigkeit σ ; Ladungsträgerkonzentrationen n, p in den Bändern; Beweglichkeit; Spezifischer Widerstand; Diffusionströme J_{diff} ; Gesamtstrom im Halbleiter.

Nichtgleichgewicht und Injektion: Rekombination und Generation; Quasi-Fermi-Niveaus (QFN oder Imref).

Elektrostatik des pn-Übergangs: Prinzip der pn-Diode; Ladungsträgerkonzentrationen im Gleichgewicht; Diffusionsspannung V_{bi} ; elektrisches Feld \mathcal{E} , Potential φ , Raumladung ρ_0 ; Kenngrößen des pn-Übergangs.

Ströme im pn-Übergang: Feld- und Diffusionsströme; Kennlinie des idealen pn-Überganges; Kapazität, Kleinsignalwiderstand und Kleinsignalersatzschaltbild des pn-Übergangs; Grenzen der idealen Diodentheorie.

Anhang: Ergänzungen zur Vorlesung: Photonenenergie und Wellenlänge von Strahlung; Messung der Bandlücke E_g ; Temperaturabhängigkeit der Bandlücke; Fermi-Niveaus des extrinsischen Halbleiters bei unbekannter Ladungsträgerkonzentration; Sättigungsgeschwindigkeit v_{sat} ; Einfluss der Dotierung(-shöhe) auf μ_n, μ_p ; Einfluss der Temperatur auf μ_n, μ_p .

2.2 Vorlesung **Solid State Electronics**

Band Model of Semiconductors: Band gap E_g and conductivity; electron concentration in conduction band.

Free Electrons as Waves: Particle properties of electrons; Davisson and Germer's experiment (1927); Bragg's diffraction condition; de Broglie's hypothesis; small and large particles and solids; condition for observation of wave properties; breakdown of classic wave/particle picture; structure analysis of solids; wave function ψ of de-Broglie waves (particle waves); Schroedinger's equation; free electron revisited in view of Schroedinger equation.

Electrons in Idealized Solids: One-dimensional potential box of size L (particle in a box); electrons in three-dimensional potential well; Fermi-distribution.

Electrons in Real Crystals: Bloch waves; band structure of some important semiconductors; the "Brillouin-Zone", reciprocal lattice vectors; allowed k -values; states per band; empty and full bands.

Band Structure and Band Model: Band structure of Si, Ge, GaAs; three-dimensional delineation; from band structure $E(k)$ to band model/diagram; metal, semiconductor, isolator; direct and indirect semiconductors; moving electrons; particle momentum p_p and pseudo-crystal momentum p_k ; holes.

Emission of Electrons from Solids: Work function $q\phi_A$, electron affinity q_x ; thermal emission; tunneling, photoemission; current/voltage curve;

A1. *Proof of the Richardson-Dushman-Equation.*

2.3 Vorlesung **Optoelectronic Devices and Circuits**

Introduction – What is Optoelectronics? Overlap of optoelectronics with classic areas; optical regime; scheme of an optical communication system; what is light?

Basic Physics: Simple equations: reflectance, absorbance, transmittance; refraction and total internal reflection; reflectance r_ϕ , transmittance t_ϕ for $\Theta_i = 0$.

Thermal Radiation: Black body radiation (Kirchhoff's radiation law, Planck's radiation law, Wien's displacement law, Stefan-Boltzmann law); grey body radiation; selective body radiation of a semiconductor.

Coherence: Definition; length of a wave train; the frequency spectrum of a wave train.

Semiconductor Basics: Energy bands and Fermi function (wave vector k , band structure $E(k)$, limited range of k -values, Brillouin zone, crystal momentum p_k , impulse p_e , direct and indirect bandgap semiconductors).

Excitation and Recombination Processes in Semiconductors: Introduction – What is luminescence? Absorption of radiation in semiconductors; carrier recombination in semiconductors.

Light Emitting Diodes: Working principle; emitted spectrum of an LED; materials for LEDs (and lasers); emission efficiency of LEDs.

Semiconductor Lasers: Working principle; laser components; ratio of induced (stimulated) to spontaneous emission; gain of a laser (first general laser condition); the resonator; first lasing condition for semiconductor lasers;

second lasing condition for a semiconductor laser; heterojunctions, heterostructures; light guiding in semiconductor lasers; stripe contact laser; laser modes; gain in a semiconductor laser; modern semiconductor lasers.

Glass Fibres: Advantages of glass fibers; fiber configurations; step-index-, graded-index- and mono-mode fibers; dispersion and attenuation in glass fibers.

Photodetectors: Introduction, general considerations; properties and specifications of photodetectors; photoconductors; photodiodes; photodiodes with internal gain: avalanche photodiodes (APDs); materials and detector configurations.

2.4 Vorlesung *Photovoltaics*

Energy Data: Energy units and energy content; consumption of Germany (2000); carbon dioxide creation; mean power for a German.

The Solar Spectrum: The sun as a black body; terrestrial solar spectrum.

Potential of Solar Radiation: Theoretical potential; technical potential of solar energy world wide; technical potential of solar energy in Germany.

The Principal Functions of Photovoltaic Systems.

Generation and Recombination in Semiconductors: Absorption of radiation in semiconductors; recombination.

Basic Semiconductor Equations: Currents in semiconductors; generation and recombination.

pn-Junctions: The *pn*-junction in thermal equilibrium; *pn*-junction under applied bias; the *pn*-junction solar cell under illumination.

Current/Voltage-Curve of Solar Cells: Characteristic values and equivalent circuit of the ideal solar cell; equivalent circuit and characteristic data of a real solar cell.

Maximum Efficiency of Solar Cells: Experimental limits; loss processes; radiative efficiency limit after Shockley & Queisser.

Preparation of Crystalline Silicon: Single crystalline silicon wafers; polycrystalline silicon wafers.

Technology of Crystalline Silicon Solar Cells: Screen printing technology; high efficiency technology.

Amorphous Silicon Solar Cells: Why thin-film solar cells; material properties of amorphous silicon; Staebler-Wronski effect; structure of an a-Si:H solar cell; preparation of a-Si:H solar cells; module and cell efficiencies; products you can buy.

Cu(In, Ga)Se₂ Solar Cells: Material properties of Cu(In,Ga)Se₂; structure of ZnO/CdS/Cu(In, Ga)Se₂ heterojunction solar cell; variation of the composition of Cu(In, Ga)(S, Se)₂ (alloying); preparation of Cu(In, Ga)Se₂ solar cells; cell and module efficiencies; new developments.

2.5 Vorlesung **Energiewandlung**

Einführung: Energie: Grundbegriffe; Energiewandlungskette, Energieträger.

Kernenergie: Grundlagen: Kernkraftwerke in Deutschland und weltweit,

Atomkerne, Massendefekt, Energiegewinn durch Spaltung und Fusion, Kernumwandlungen; Kontrollierte Kernspaltung: Kettenreaktion und kritische Masse, prompte und verzögerte Neutronen, Aufbau eines Kernreaktors, Energiebilanz, Kritikalität und Reaktivität, Moderatoren, Steuerung der Kettenreaktion.

Thermodynamik: Definitionen: Energie, chemisches Potential, Verbrennung,

Heizwert und Brennwert, Entropie, thermodynamische Potentiale;

Zustandsgleichungen: Ideales Gas, reale Gase; Kreisprozesse: Carnot-Prozess, weitere Kreisprozesse; Wärmekraftmaschine/Kraftwärme-maschine; Exergie; Hauptsätze der Thermodynamik; kWh(el) und kWh(therm).

Direkte Nutzung der Sonnenenergie: Der AM-Wert, das Sonnenspektrum, globale, diffuse und direkte Strahlung, Jahresgang der Globalstrahlung in Deutschland, die Sonne als schwarzer Strahler; solarthermische Energiewandlung: Niedertemperaturkollektoren, selektive Absorber, selektive Abdeckung, Kollektorwirkungsgrad; Photovoltaik: Halbleiter und Solarzellen, Lichtabsorption, Kennlinie und Wirkungsgrade, Verluste in realen Solarzellen, Dünnschichtsolarzellen, Entwicklung der Photovoltaik.

Indirekte Nutzung der Sonnenenergie: Wasserkraft: Beitrag zur Stromerzeugung,

Leistung eines Wasserkraftwerks, Kraftwerksarten, Turbinenarten;

Windenergie: Leistung des Windes, maximaler Wirkungsgrad eines Rotors, Widerstands- und Auftriebsläufer, Bauformen von Windkraftwerken..

Chemische Umsetzung elektrischer Energie: Galvanische Elemente;

Primärelemente: Batterietypen, Anwendungen; Akkumulatoren: der Bleiakkumulator und andere Typen; Kondensatoren: Vergleich Batterie/Kondensator, Elektrolyt- und Superkondensator; Energiedichten von Batterien, Akkus und Kondensatoren; Brennstoffzellen: Funktionsprinzip, Typen und Typenvergleich.

2.6 Vorlesung ***Lasers and Light Sources***

The Human Eye: Anatomy of the human eye; refracting power D of the human eye; near point, far point; focusing problems; rods, cones; color vision; color deficiency.

Light and Color: Light sensitivity of the human eye; CIE color matching functions[^]; color coordinates X, Y, Z and color chromaticity coordinates x, y, z; chromaticity diagram; colcor mixing.

Photometry and Colorimetry: Energetic quantities of radiation and irradiation; visual quantities of light and illumination.

Incoherent Light Sources: Black body radiation; gray body radiation; selective body radiation of a semiconductor; emissivity of non-black bodies; incandescent lamps; gas discharge light sources.

Light Emitting Diodes: Working principle; the emitted spectrum of an LED; materials for LEDs (and lasers); emission efficiency of LEDs; organic light emitting diodes (OLEDs).

Lasers: Fundamental processes; occupation probability in thermodynamic equilibrium; microscopic analysis; set-up of a laser; optical resonator; line width; laser types; semiconductor lasers.

2.8 Praktika. / *Laboratory courses*

Grundlagenpraktikum *Physikalische Elektronik* im Vorstudium, WS + SS

4 Versuche: Lichtemittierende Dioden (LED), Laserdiode, Farbfernsehtechnik, Photovoltaik mit Netzeinspeisung.

Praktikum *Elektrophysik* im Hauptstudium, SS

a) Praktikum Photovoltaik:

7 Versuche: Dünnschichtsolarzellen aus Verbindungshalbleitern, Teil 1:
Solarzellenpräparation / Aufdampfanlage;
Dünnschichtsolarzellen aus Verbindungshalbleitern, Teil 2:
Absorbercharakterisierung / REM mit EDX;
Elektrische Charakterisierung von Dünnschichtsolarzellen (CIS),
Strom-Spannungs-Kennlinie, Bestimmung der Bandlücke E_g ,
spektrale Quantenausbeute;
Dünnschichtsolarzellen aus amorphem Silicium,
Solarzellenpräparation / CVD;
Jahresenergieerträge verschiedener PV-Technologien in Europa,
 η/E -Messungen an mono-c-Si-, multi-c-Si-, a-Si- und CIS-Zellen,
Berechnung der Jahresenergieerträge für die Standard-Europa-
Einstrahlungsverteilung;
Verschaltung von Zellen zu Modulen, Abschattungsprobleme,
Bypass- und Blockierdioden;
Inselsystem, Solar Home System, Aufbau und Funktionstest mit
SHS-Tester, Simulationsprogramm;

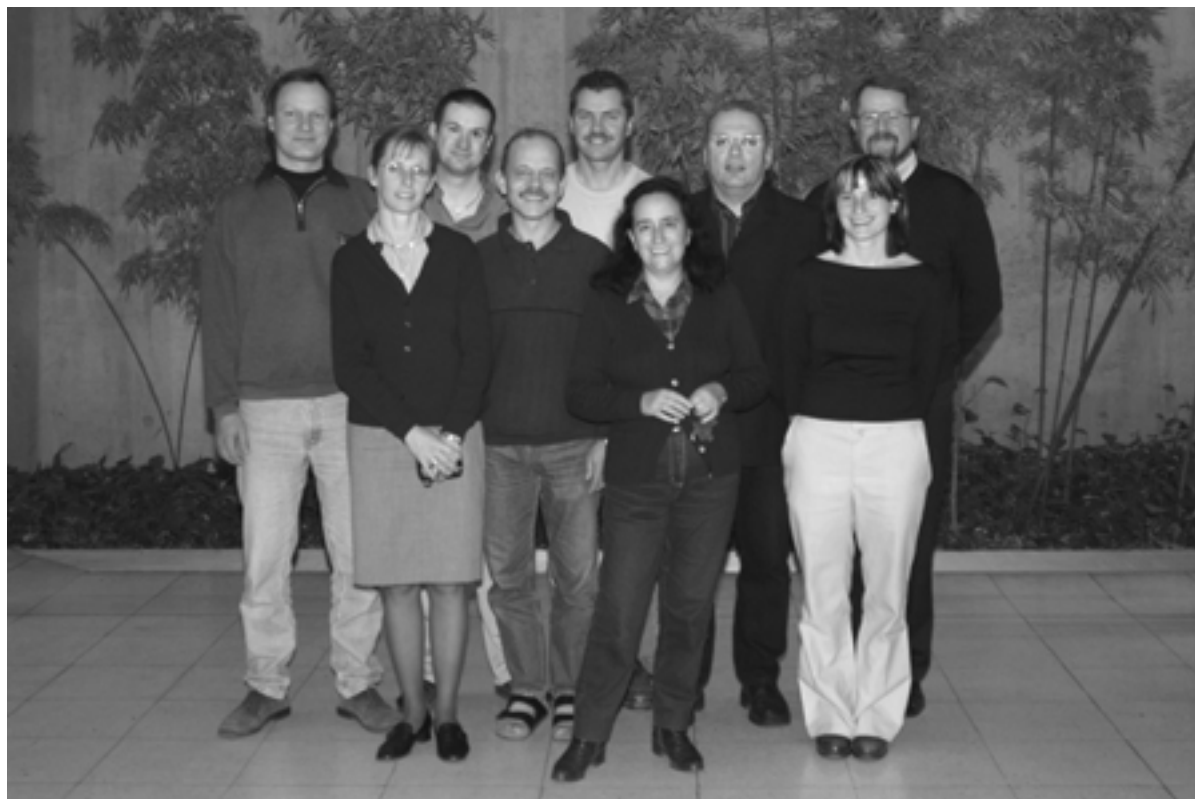
b) Praktikum Mikroelektronik (mit Institut für Mikroelektronik Stuttgart):

9 Versuche: Bauelementesimulation mit Atlas (Silvaco), device-Simulation el.
Parameter;
Diffusion / Oxidation;
Ionenimplantation / Ionen-Projektionslithographie;
Lithographie;
Vakuumtechnik / Metallisierung;
Materialcharakterisierung / REM / EDX / EBIC;
Schaltungssimulation mit SPICE;
Elektr. Charakterisierung / $/V/CV..$;
IC-Lab (digitaler Schaltungsentwurf, Hierarchie, Netzlisten,
Verifikation).

3 Menschen am ipe / People at the ipe



3.1 Verwaltung, Werkstatt und Institutsleitung / Administration, Workshop, and Head of the Institute



Verwaltung, Werkstatt und Institutsleitung / *Administration, Workshop, and Head of the Institute*: Von links (*from left*): Markus Schubert, Christine von Rekowski, Werner Wille, Jürgen Köhler, Anton Riß, Isabel Kessler, Jürgen Werner, Lydia Diegel, Fritz Pfisterer.

3.2 Gruppe Silicium / Group Silicon

Gruppenleiter/Group Leader: MARKUS SCHUBERT

Mitarbeiter/Collaborators: Lukas Alberts, Anas al Tarabsheh, Christopher Berge, Willi Brendle, Klaus Brenner, Caroline Carlsson, Yasuaki Ishikawa, Christiane Köhler, Brigitte Lutz, Michail Rakhlin, Minji Zhu (and those who left in 2003: Anne Carlsson, Cecilia Craff Castillo, Christian Gemmer, Martin Rojahn, Thomas Wagner, Maoxiang Yi)

Die Arbeitsgruppe "Silicium" des *ipe* entwickelt elektronische Bauelemente auf der Basis von Silicium. Da wir hierzu vorwiegend dünne Schichten verwenden, können Solarzellen, Sensoren und andere Bauelemente direkt auf flexiblen Trägermaterialien hergestellt oder auf biegsame Folien transferiert werden. Wir arbeiten mit allen Modifikationen des Siliciums von einkristallinen Wafern und Dünnschichten bis hin zu nanokristallinen und amorphen Filmen. Unsere Forschungs- und Entwicklungsprojekte konzentrieren sich auf die Anwendung dünner Halbleiterschichten in Solarzellen. Die "integrierte Photovoltaik" (*ipV*) nutzt die mechanische Flexibilität der Dünnschichtzellen, um sie in Kleidung zu integrieren und damit die elektrische Energie zum Betrieb mobiler Kleingeräte bereit zu stellen. In Kooperation mit dem Institut für Mikroelektronik Stuttgart (ims-chips) bietet das Praktikum "Device and Microchip Technologies" Einblick in das Design und die Herstellung moderner Mikroelektronik-Bauelemente. Wafertechnologie und Dünnschichttechnik unterstützen und befruchten sich gegenseitig, beispielsweise in der Entwicklung von "Thin-Film-on-CMOS"-Kameras oder Positionssensoren.

The silicon group at *ipe* develops electronic devices based on silicon. We predominantly use thin films. Hence, solar cells, sensors and other devices can directly be deposited onto flexible substrates, or later transferred to bendable foils. We employ all modifications of silicon, from single-crystalline wafers and thin films to nanocrystalline as well as amorphous material. Our main activities in research and development aim at making the best use of thin films for photovoltaic applications. "Integrated Photovoltaics" (*ipV*) utilizes the mechanical flexibility of our thin film solar cells for integrating them with clothes and accessoires to provide electric power for mobile communication and entertainment electronics. Cooperating with the Institute of Microelectronics Stuttgart (ims-chips), we offer a laboratory course in "Device and Microchip Technologies" which gives insight into design and manufacturing of modern microelectronic devices. Wafer-based technology and thin film processing mutually enhance each other, e.g. in developing "Thin-Film-on-CMOS" cameras and position sensors.



Gruppe Silicium / *Group Silicon*: Von links (*from left*): Lukas Alberts, Christopher Berge, Brigitte Lutz, Willi Brendle, Minji Zhu, Christiane Köhler, Markus Schubert, Michail Rakhlin, Klaus Brenner, Caroline Carlsson, Yasuaki Ishikawa, Anas al Tarabshah.

Im Lauf des Jahres 2003 konnten wir die gesamte Silicium-Prozesstechnologie von 100 mm auf 150 mm Scheibendurchmesser umstellen. Die Abbildung zeigt W. Brendle an der neu eingerichteten Nassprozessbank.

In 2003, we were able to upgrade all silicon processing equipment from 100 to 150 mm wafer diameter. This photograph shows W. Brendle working with the new wet bench.



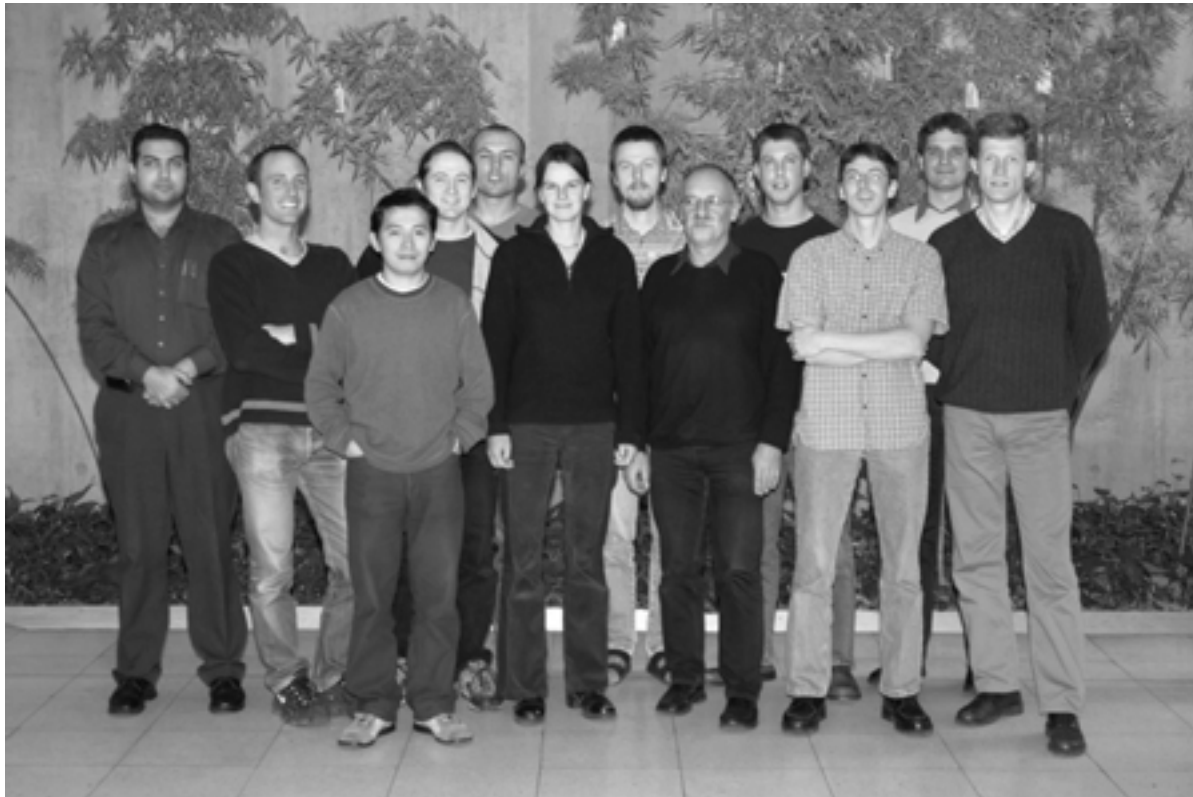
3.3 Gruppe Verbindungshalbleiterschichten / Group Compound Semiconductor Films

Gruppenleiter/Group Leader: HANS-WERNER SCHOCK

Mitarbeiter/Collaborators: George Hanna, Adrian Harding, Kay Orgassa, Philip Jackson, Nguyen Hong Quang, Osama Tobail, Thomas Schlenker, Thomas Schlötzer, Holm Wiesner (and those who left in 2003: Daniel Bäder, Kerstin Gebhardt)

Die Gruppe *Verbindungshalbleiterschichten* entwickelt vor allem Dünnschichtsolarzellen mit Heterostrukturen aus ternären Halbleiterverbindungen wie CuInSe_2 (CIS) und verwandten Materialien als Absorberschichten und ZnO als Fensterschicht. Herstellungsverfahren für die Dünnschichten sind eigens hierfür entwickelte Aufdampf- und Sputterprozesse, sowie Abscheidungen aus chemischen Lösungen. Hilfsmittel zur Analyse der Schichten und der Heterostrukturen sind Photoelektronenspektroskopie, Rasterelektronen-mikroskopie sowie Röntgenspektroskopie und Röntgenbeugung. Entwicklungsziele sind die Steigerung der Effizienz der Solarzellen auf 20%, die Weiterentwicklung von Solarzellen aus Verbindungen mit Bandabständen größer als 1,3 eV und entsprechend hoher Leerlaufspannung, die Optimierung von Cd-freien Frontelektroden und darüber hinaus strahlungsbeständige Dünnschichtsolarzellen mit geringem Gewicht für die Raumfahrt. Forschungsthemen sind die generellen Eigenschaften von komplexen Verbindungshalbleitern, insbesondere die Zusammenhänge zwischen Eigendefekten, Verunreinigungen und elektrischen und optischen Eigenschaften.

The *Compound Semiconductor Films* group mainly investigates thin-film solar cells based on ternary compound semiconductors such as CuInSe_2 and related compounds. For the deposition of thin films, special coevaporation and sputtering processes as well as chemical processes are designed. Main tools for the optimization of heterostructures are photoelectron spectroscopy, scanning electron microscopy, well as X-ray spectroscopy and X-ray diffraction. Goals of the developments are solar cells with an efficiency of about 20 %, the improvement of solar cells with band gaps in excess of 1.3 eV for high-voltage cells, the optimization of Cd-free front electrodes and, furthermore, radiation resistant, lightweight solar cells for space applications. Topics for research are the general properties of complex compound semiconductors, in particular the relations between native defects, impurities, and the electrical and optical properties.



Gruppe Verbindungshalbleiterschichten / *Group Compound Film Semiconductors:*
Von links (*from left*) : Osama Tobail, George Hanna, Nguyen Quang, Thomas
Schlötzer, Thomas Schlenker, Gerda Gläser, Holm Wiesner, Hans-Werner Schock,
Andreas Strohm, Kay Orgassa, Adrian Harding, Philip Jackson.

Hochvakuum-Beschichtungsanlage zur Herstellung von CIGS-Solarzellen-Heterostrukturen.

High vacuum deposition system for the fabrication of CIGS-based heterojunction solar cells.



3.4 Gruppe Laserprozesse / *Group Laser Processing*

Gruppenleiter/Group Leader: JÜRGEN R. KÖHLER

Mitarbeiter/Collaborators: Ainhoa Esturo-Breton (and who left in 2003: Jakob Demir)

Die Gruppe *Laserprozesse* entwickelt neue Technologien zur Laserprozessierung der am *ipe* verwendeten einkristallinen und polykristallinen Halbleiter. Hierzu zählen die Strukturierung der Halbleiter, deren Kristallisation und Rekristallisation sowie die Laser-Dotierung zur Herstellung von Emittern und Rückseitenkontakte für einkristalline Silicium-Solarzellen. Im Vordergrund unserer Arbeiten stehen Grundlagenuntersuchungen zur Laserdotierung von einkristallinem Silicium. Entwicklungsziele sind die Erhöhung des Durchsatzes bei der laserunterstützten Emitterdotierung sowie die Steigerung der Wirkungsgrade von 100 mm x 100 mm großen einkristallinen Silicium-Solarzellen auf über 17%.

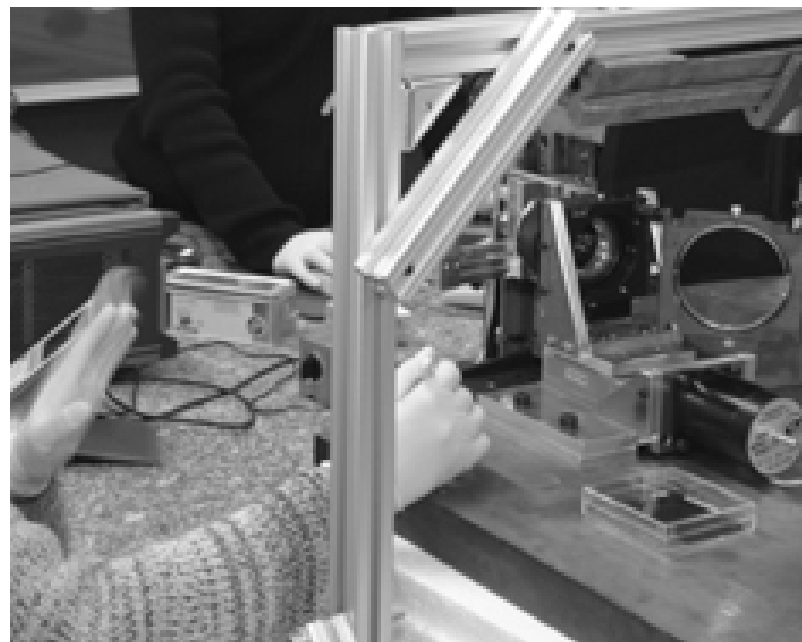
The *laser processing* group explores new technologies for laser processing of monocrystalline and polycrystalline semiconductors. Examples are laser structuring, laser annealing, laser crystallization and laser doping of monocrystalline silicon. The main topic of our research work is the investigation of the fundamental processes involved in a pulsed laser doping process for the preparation of n⁺-doped emitters on monocrystalline silicon wafers. Development goals are the increase of the throughput rate of the laser doping process as well as the increase of the efficiency of 100 mm x 100 mm sized monocrystalline silicon solar cells to more than 17%.



Gruppe Laserprozesse / *Group Laser Processing* : Von links (*from left*) : Mawuli Ametowobla, Ainhoa Esturo-Breton, Jürgen Köhler

Einbau einer Probe zur anschließenden Laser-Prozessierung.

Fitting of a sample for subsequent laser-processing.



3.5 Gruppe CIS-Technologie und Oberflächenanalyse / Group CIS Technology and Surface Analysis

Gruppenleiter/Groupleader: GERHARD BILGER

Mitarbeiter/Collaborators: Leo Bauer, Lorenz Eisenmann, Peter Grabitz, Denis Kühnle, Viktor Laptev, Martin Wagner (and who left in 2003: Thomas Dolch)

Die bei der *Oberflächenanalyse* angewandten Methoden sind die Sekundärionen-Massenspektrometrie (SIMS) sowie die Röntgen- und Ultraviolett-Photoelektronen-Spektrometrie (XPS, UPS). Die Analytik unterstützt die Gruppen, die Forschung und Entwicklung an Materialien für die Photovoltaik und Sensorik am *ipe* betreiben. Nach außen werden diese Analytikmethoden als Dienstleistungen für die Industrie und andere Institute angeboten. Als sehr empfindliche Methode weist SIMS alle Elemente und deren Verbindungen bis in den ppb-Bereich nach. Tiefen- und ortsaufgelöste Analysen zeigen den Verlauf von Elementverteilungen in einer Schichtfolge und/oder deren laterale Verteilung. XPS-Analysen, empfindlich bis in den 0,1 Atom%-Bereich, sind quantitativ und geben Auskunft über Bindungszustände der Elemente. Die extrem oberflächensensitive Methode weist noch Oberflächenbedeckungen von 1/10 einer Monolage nach. Mit UPS wird die Valenzbandstruktur von Festkörpern untersucht. Bei der *CIS Technologie* liegt die Verantwortung für die Durchführung routinemäßiger Schichtpräparationen und den Unterhalt der dafür notwendigen Infrastruktur.

For *Surface Analysis* the methods applied are Secondary Ion Mass Spectrometry (SIMS) and X-ray- and Ultraviolet-Photoelectron Spectrometry (XPS, UPS). These methods support the work of the groups at the Institute of Physical Electronics involved in research and development of materials for photovoltaics and sensors. Analyses are also offered as a service to other institutes and to industry as well. The method SIMS is very sensitive to the detection of all elements and their compositions with concentrations down to the ppb region. SIMS detects the distribution of elements in layers laterally resolved and/or in their depth. The analysis technique XPS is quantitative down to a concentration of 0.1 atomic % and gives information about the chemical binding state. XPS detects surface coverages down to 1/10 of a monolayer. The method UPS is applied to study the structure of the valence band in solids. *CIS Technology* includes the routine preparation of CuInSe₂ thin films for solar cells and the maintenance of the infrastructure necessary for it.



Gruppe CIS Technologie und Oberflächenanalyse / *Group CIS Technology and Surface Analysis:* Von links (*from left*) : Peter Grabitz, Dennis Kühnle, Leo Bauer, Viktor Laptev, Gerhard Bilger, Andreas Strohm, (nicht abgebildet / *not present*: Martin Wagner)

Probenpositionierung mit dem Manipulator im Sekundärionen-Massenspektrometer.

Positioning of samples for secondary ion mass analysis.



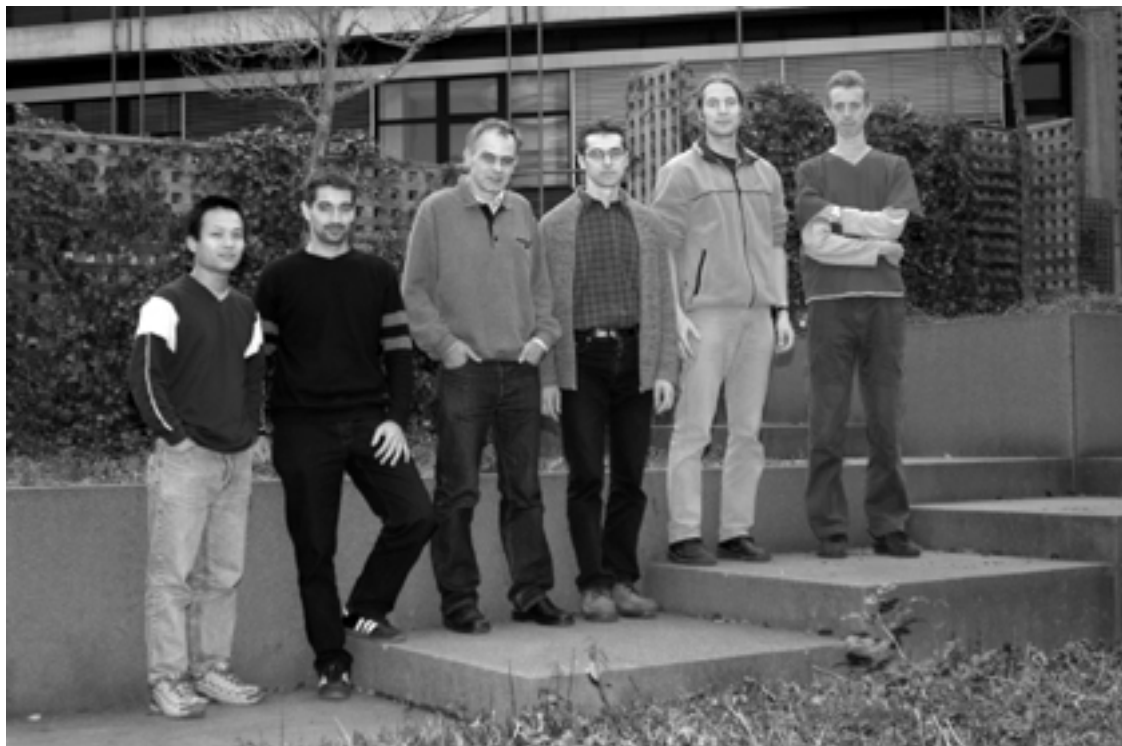
3.6 Gruppe Bauelementanalyse / *Group Device Analysis*

Gruppenleiter/Group Leader: UWE RAU

Mitarbeiter/Collaborators: Julian Mattheis, Viet Nguyen, Kurt Taretto-Zeyen, Johannes Rostan, Mircea Turcu (and those who left in 2003: Kristin Weinert, Gregor Kron).

Die Gruppe *Bauelementanalyse* befaßt sich mit der elektrischen und optischen Charakterisierung sowie der numerischen Simulation von Solarzellen basierend auf CdS/Cu(In,Ga)Se₂ und a-Si:H/c-Si Heterostrukturen sowie von Farbstoff-Solarzellen auf der Basis von nano-porösem TiO₂. Ziel unserer Aktivitäten ist ein grundlegendes Verständnis der Funktionsweise dieser Bauelemente, des Einflusses der Präparationsbedingungen und des Designs des Bauteils auf seine Leistungsfähigkeit. Wir benutzen elektrische Analysemethoden wie Strom-Spannungsmessungen, Admittanzspektroskopie und Transienten-Spektroskopie tiefer Störstellen (DLTS). Messungen der internen Quantenausbeute und Photolumineszenz dienen zur Untersuchung der elektro-optischen Eigenschaften der Materialien. Die experimentellen Resultate werden mit quantitativen, numerischen wie analytischen, Modellen verglichen, um ein kohärentes Verständnis der Bauelemente zu erhalten.

The *device analysis* group is concerned with the electrical and optical characterization and with the numerical simulation of large-area electronic devices such as solar cells based on CdS/Cu(In,Ga)Se₂ and a-Si:H/c-Si heterojunctions as well as dye-sensitized solar cells based on nano-porous TiO₂. We focus on a fundamental understanding of the working principle of these devices, the influence of preparation conditions and device design on the performance and, finally, on the improvement and optimization. Electrical analysis is performed with the help of current-voltage measurements, admittance spectroscopy, deep level transient spectroscopy (DLTS), and similar methods. Electro-optical analysis comprises measurements of internal quantum efficiency, optical transmittance and reflectance, photoluminescence, etc. The quantitative and coherent interpretation of these experimental results requires detailed modeling and simulation.



Gruppe Bauelementanalyse / *Group Device Analysis* : Von links (*from left*) : Viet Nguyen, Johannes Rostan, Uwe Rau, Mircea Turcu, Julian Mattheis, Kurt Taretto.

Kontaktierung von Solarzellen zur anschließenden elektrischen Charakterisierung.

Preparation of solar cells for electrical characterisation.



4 Wissenschaftliche Beiträge / *Scientific Contributions*

4.1 Role of the Cu(In,Ga)Se₂ Surface Defect Layer for the Performance of ZnO/CdS/Cu(In,Ga)(Se,S)₂ Solar Cells

Author: U. RAU

In collaboration with: M. Turcu

The surface properties of Cu(In,Ga)Se₂ (CIGS) polycrystalline thin films are especially important as this surface becomes the active interface of the completed ZnO/CdS/CIGS heterojunction solar cells. Especially the question, whether the type inversion of the Cu(In,Ga)Se₂ surface defect layer (SDL) of as-grown films [1,2] and of completed heterojunction devices results from an n-type doping of the surface (doping model) or from shallow surface donors that pin the Fermi-level close to the conduction band (pinning model), is still not finally cleared.

The present work [3] uses numerical device simulations to study the implications of these two pictures on the performance of the solar cell. The simulated device structure consists of the doped and intrinsic ZnO window, the CdS buffer, the 50 nm thick surface defect layer SDL, and the chalcopyrite CIGS absorber. Figure 1 shows the calculated efficiency η and open circuit voltage V_{OC} of the device as a function of doping concentration in the SDL (doping model, Fig. 1a and 1b) and as a function of density of interface states at the CdS/SDL interface (pinning model, Fig. 1c and 1d). The internal valence band offset ΔE_V between the SDL and the chalcopyrite material is taken as a parameter and an additional band gap profile (half symbols) with a gradual lowering of the valence band edge of the absorber towards the interface with CdS is also considered. Without band gap widening (open symbols), high n-type bulk doping concentration of 10^{17} cm^{-3} in the SDL (a and b), or Fermi level pinning at the interface with CdS (c and d) with interface state densities of around $10^{13} \text{ cm}^{-2}\text{eV}^{-1}$ are necessary to improve the calculated efficiency η and the open circuit voltage V_{OC} of the device. The internal valence band offset $\Delta E_V = 0.2 \text{ eV}$ (full symbols) or the graded band gap profile (half symbols) makes the calculated η and V_{OC} of the device more independent from the n-type doping in the SDL (in the doping model), or from the density of interface states at the CdS/SDL interface (in the pinning model). This is because the band gap widening towards the absorber surface increases the energy barrier ϕ_b at the CdS/SDL interface and therefore diminishes the interface recombination

[4]. The recombination in the space charge region of the absorber becomes thus more prominent, a situation characteristic to devices based on Cu-poor chalcopyrite absorbers. In turn, devices based on absorbers prepared under Cu-rich conditions show relatively low interface barriers and are therefore assumed to be dominated by recombination at the CdS/absorber interface [4,5]. Thus, only such devices *without* band gap widening need a high *n*-type doping concentrations in the SDL or Fermi level pinning at the CdS/SDL interface for the minimization of interface recombination. In turn, in high-efficiency Cu-poor devices that posses the SDL with a band gap widening towards the CIGS surface maintain an improved device efficiency and open circuit voltage irrespective of doping concentrations in the SDL or Fermi-level-pinning at the CdS/SDL interface.

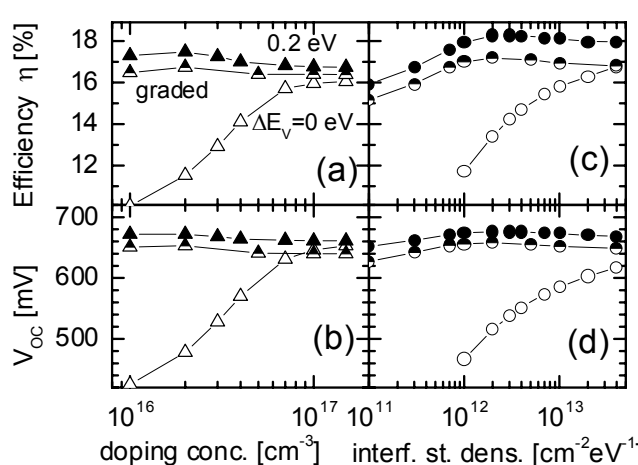


Figure 1: Calculated efficiency η and open circuit voltage V_{oc} for the n-type SDL (doping model, a and b) and for the SDL with Fermi-level pinning (c and d). An internal valence band offset $\Delta E_v = 0.2 \text{ eV}$ (full symbols) or a graded structure (half symbols) makes the parameters, to a first order, independent from the doping concentration in the SDL (within the doping model) or from the density of states at the CdS/SDL interface (within the pinning model). The devices with no internal band offset (open symbols) require high n-type doping or Fermi level pinning.

References:

- [1] D. SCHMID, M. RUCKH, F. GRUNWALD, AND H. W. SCHOCK, J. Appl. Phys. **73**, 2902 (1993).
- [2] M. MORKEL, L. WEINHARDT, B. LOHMÜLLER, C. HESKE, E. UMBACH, W. RIEDL, S. ZWEIGART, AND F. KARG, Appl. Phys. Lett. **79**, 4482 (2001).
- [3] U. RAU AND M. TURCU, Mat. Res. Soc. Conf. Proc. **763**, B8.8 (2003).
- [4] M. TURCU AND U. RAU, J. Phys. Chem. Solids **64**, 1591 (2003).
- [5] M. TURCU, O. PAKMA, AND U. RAU, Appl. Phys. Lett. **80**, 2598 (2002).

4.2 Efficiency Limitations of Cu(In,Ga)Se₂ Solar Cells by Electronic Inhomogeneities

Author: J. H. WERNER

In collaboration with: J. Mattheis, U. Rau

World-best solar cells of more than 19 % efficiency and best commercial modules from Cu(In,Ga)Se₂ (CIGS) films are fabricated by co-evaporating the constituting elements onto glass substrates. As a result one obtains polycrystalline films of about 2 µm thickness with grain sizes around 0.5 µm. Thus, the films have a high structural disorder due to grain boundaries, dislocations and point defects. In addition, the films are highly compensated and “doped” with Na, O, Cd and other impurities. It is, therefore, evident that such films as well as their interfaces and surfaces *must* be electronically inhomogeneous. Nevertheless, the modeling of the electronic properties of CIGS solar cells, thus far, has been restricted to models that assume lateral electronic homogeneity.

Our research, which is based on earlier models for electronic inhomogeneities at Schottky contacts and silicon grain boundaries [1, 2], showed that the efficiency of the world-best CIGS solar cells is limited by potential fluctuations within the *bulk* of the polycrystalline CIGS films. Figure 1 shows such potential fluctuations at the conduction and valence band edge. These fluctuations are caused by

- i) spatial *compositional* fluctuations due to variations of the composition, stoichiometry and strain by variations of the Ga/In- and Cu/In-ratio.
- ii) *electrostatic* fluctuations due to the spatial distribution of charges at and within grain boundary planes, dislocations, as well as due to the statistical distribution of bulk defects and of the doping atoms.

Our novel model takes into account both kinds of potential fluctuations [3, 4]. The compositional potential fluctuations are quantified in optical measurements and have a Gaussian standard deviation of 55 meV [3]. If there were only such compositional band gap fluctuations, the present diffusion length of about 3 µm for electrons in CIGS would allow for solar cell efficiencies of about 26 % [4].

Instead of 26 %, the world-best cells reach 18 to 19 % efficiency and range thus more than 5 % below the world-best silicon solar cells which

make almost 25 %. The reason for the efficiency limitation of CIGS lies in the *electrostatic* potential fluctuations. Spatially distributed charges at electronic defects give rise to electrostatic fluctuations, resulting in an increased zero bias minority carrier concentration [4]. As a consequence, the saturation current density in the polycrystalline cells is drastically increased and the open circuit voltage is degraded. In addition, electrostatic potential fluctuations cause a diode ideality factor $n_{id} > 1$. Within our model [4], $n_{id} > 1$ in the current/voltage curves is a measure for the electronic homogenization of the sample upon the application of either a bias voltage or illumination. From the ideality factor $n_{id} = 1.5$ we derive Gaussian (zero bias) electrostatic potential fluctuations with a standard deviation of 140 meV. Increasing the efficiency of CIGS cells above 20 % requires a drastic reduction of such electrostatic potential fluctuations.

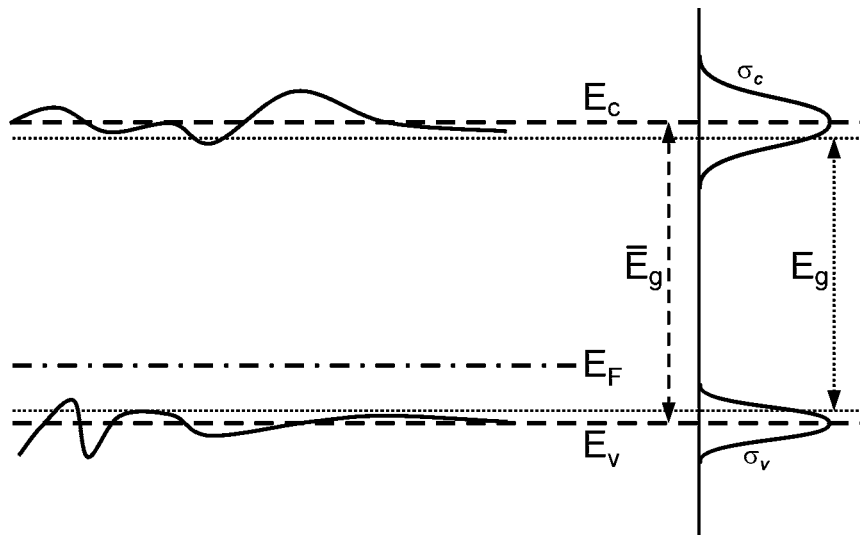


Figure 1: Potential fluctuations (modelled by Gaussian distributions) in the conduction and valence band result in spatial band gap fluctuations. These band gap fluctuations show up in a lowered efficiency.

References:

- [1] J. H. WERNER, Inst. Phys. Conf. Ser. **104**, 63 (1989).
- [2] J. H. WERNER AND H. H. GÜTTLER, J. Appl. Phys. **69**, 1522 (1991); Physica Scripta **T39**, 258 (1991).
- [3] U. RAU AND J. H. WERNER, unpublished.
- [4] J. H. WERNER, J. MATTHEIS AND U. RAU, unpublished.

4.3 Grain Growth in Thin Cu(In,Ga)Se₂ Films

Author: T. SCHLENKER

In collaboration with: M. Luis Valero, H. W. Schock, J. H. Werner

Grain size is an important parameter for the quality of polycrystalline thin films. Grain growth in thin films occurs during deposition or during post-deposition processing. The substrate heater in an ultrahigh vacuum chamber serves to perform annealing steps with Cu(In,Ga)Se₂ (CIGS) films of 1 μm thickness. Ultra high resolution scanning electron microscopy (SEM) visualizes the cross-section of the films in order to determine the average grain radius r . The theory of normal grain growth explains the increase of the average grain radius depending on the annealing time t and the annealing temperature T according to the following equation [1]:

$$r^m - r_0^m = \beta e^{\frac{-Q}{k_B T}} t, \quad (1)$$

where r_0 is the average initial grain radius in growth direction and Q the activation energy for grain boundary motion. For equiaxed grains, the exponent m is expected to have a value of 2. If the initial structure has a columnar character as in the case of (CIGS), deviations from Eq. 1 occur, that lead to exponents m with higher values [1,2]. The parameter β is a weakly temperature-dependent constant, which depends on the grain geometry and the average grain boundary energy per unit area of grain boundary.

In a first series, we heat the (CIGS) layers for varying times t at constant temperature T . Figure 1a and 1b show SEM micrographs of CIGS layer cross-sections before (a) and after annealing. The quantitative analysis of the average grain radius growth is plotted versus annealing period t in Fig. 1c. The fit according to Eq. 1 yields $m = 5$.

In a second series, we anneal samples with different Cu-contents of 17.9 %, 22.1 % and 25.7 % at varying T for a fixed period. Our results in Fig. 2 show that the atomic diffusion is highly temperature sensitive in the substrate temperature region in which Cu(In,Ga)Se₂ is currently processed. Thus, small temperature variations are crucial for the quality of the resulting absorber layer. In case of the 25.7 % Cu-content sample, grain growth stagnation [1] leads to deviations from the expected trend for $T \geq 570$ °C. The fits to Eq. 1 yield activation energies Q depending on Cu-content of 3.3 eV (17.9 % Cu), 3.1 eV (22.1 % Cu) and 2.9 eV (25.7 % Cu).

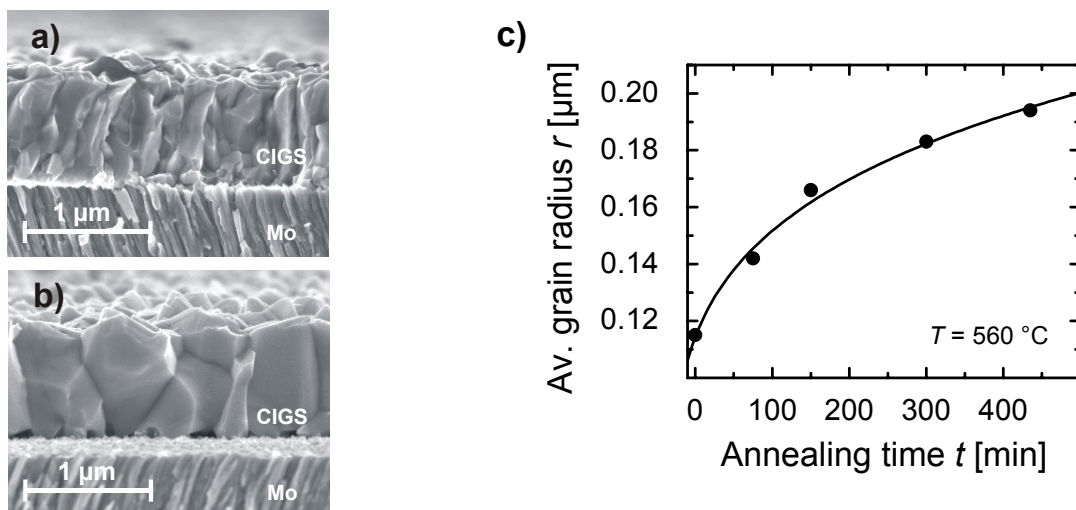


Figure 1: a,b) Scanning electron micrographs of $\text{Cu}(\text{In},\text{Ga})\text{Se}_2$ (CIGS) films on Mo substrates before (a) and after (b) annealing for $t = 3$ h at $T = 610$ °C. c) Quantitative analysis of CIGS grain growth at a constant annealing temperature $T = 560$ °C. A root function fits the measured values (solid line).

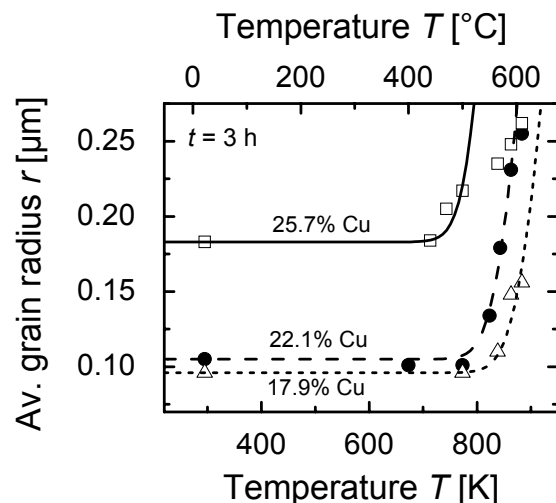


Figure 2: Average grain radii r at a constant annealing period $t = 3$ h for three samples with varying Cu-content. The Cu-content (squares, full line 25.7%, solid dots, dashed line 22.1%, triangles, dotted line 17.9%) influences the activation energy Q for grain boundary motion. Due to grain growth stagnation, the fit for the 25.7 %-Cu sample does not take into account the measured values for $T \geq 570$ °C.

References:

- [1] C. V. THOMPSON, Annu. Rev. Mater. Sci. **20**, 245 (1990).
- [2] H. A. ATWATER, C. V. THOMPSON, and H. I. SMITH, J. Appl. Phys. **64**, 5 (1988).

4.4 Influence of Film Texture on Grain Boundary Activity in Cu(In,Ga)Se₂ films

Author: G. HANNA

In collaboration with: Thilo Glatzel¹, S. Sadewasser¹, Niels Ott², H. P. Strunk², H. W. Schock, U. Rau, J. H. Werner

A preferred (220/204) crystallographic orientation (texture) of Cu(In,Ga)Se₂ (CIGS) absorber layers most probably is beneficial for the performance of finished CIGS solar cells as compared to (112) textured CIGS layers [1,2]. We study the laterally resolved electronic properties of CIGS thin films with different textures by means of Cathodo-luminescence (CL) mapping, measured in a transmission electron microscope setup, and Kelvin Probe Force Microscopy (KPFM).

Figure 1a, 1b show panchromatic CL-mappings of samples with a (112) and a (220/204) texture. The (220/204) textured sample (Fig. 1b) has a very homogenous lateral CL-intensity whereas the CL mapping of the (112) textured sample (Fig. 1a) exhibits strong contrasts in the CL-signal. Here, the light areas correspond to the grains and the dark areas to the grain boundaries (GBs) of the film. These dark areas indicate an increased non-radiative recombination at the GB of the (112) textured film. Thus, the superior properties of CIGS films with a (220/204) texture as compared to films with a (112) texture are due to a lower electronic activity of the film's GBs resulting in a lower recombination of minority carriers at the GBs.

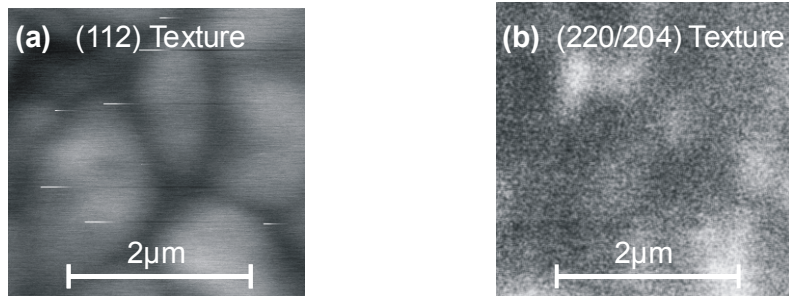
The line scans of the work function Φ across GBs in Figs. 1c, 1d yield complementary information about the electronic properties of GBs in (112) or (220/204) textured films. Note, that these scans were measured with KPFM simultaneously with the surface topography. The course of the work function Φ of the (112) textured sample (Fig. 1 (c)) exhibits a dip of more than 300 meV across the GB while at the (220/204) sample (Fig. 1 (d)) Φ shows no comparable dip at the GB but rather has a small spike. The fact that the work function Φ of the (112) textured film (Fig. 1 (c)) is significantly lower at the GB than in the grain indicates that positive charges are present at GBs of such films. Positively charged GBs in polycrystalline p-type semiconductors enhance recombination of charge carriers at GBs and, thus, negatively affect the performance of the finished solar cell [3]. In contrast, the course of Φ of

¹ Hahn Meitner Institut, Berlin, Germany

² Institut für Werkstoffwissenschaften VII, Universität Erlangen-Nürnberg, Germany

(220/204) textured films (Fig. 1(d)) indicates that the GBs either have a flat-band condition or that the GBs carry negative charges and, thus, reflect minority charge carriers which is "most desirable for polycrystalline solar cells" [3].

Cathodoluminescence Mapping:



Kelvin Probe Force Microscopy:

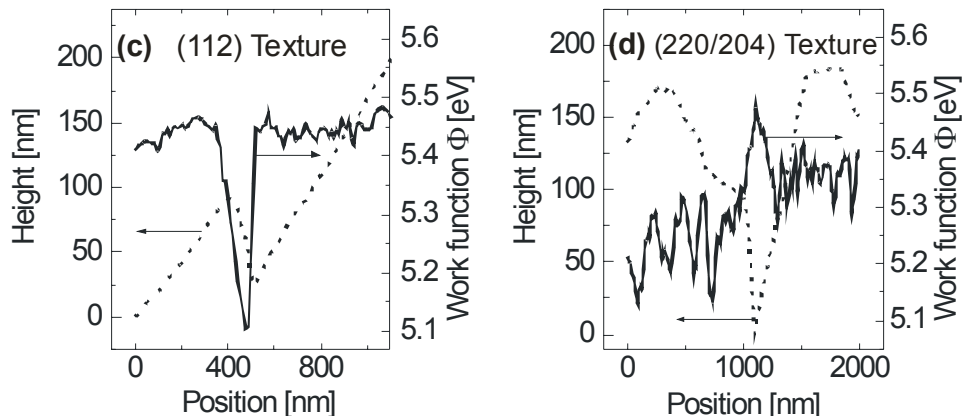


Figure 1: Panchromatic CL-mappings of (a) a (112) and (b) a (220/204) textured CIGS thin film. The CIGS layer with a (112) texture shows clear contrasts in the CL signal at grain boundaries whereas the sample with a (220/204) texture has an almost homogenous CL signal. Topography (height) of the sample's surfaces and work function Φ across a GB of (c) a (112) textured and (d) a (220/204) textured sample as determined with KPFM measurements. A strong dip of Φ marks the position of the GB in the (112)-oriented sample. In contrast to that, the work function Φ has a spike at the GB of the (220/204) textured CIGS film.

References:

- [1] M. A. CONTRERAS, B. EGAAS, K. RAMANATHAN, J. HILTNER, A. SWARTZLANDER, F. HASOON, AND R. NOUFI, *Prog. Photovoltaic Res. Appl.* **7**, 311 (1999).
- [2] S. CHAISITSAK, A. YAMADA, AND M. KONAGAI, *Jpn. J. Appl. Phys.* **41**, 507 (2002).
- [3] J. H. WERNER AND N. E. CHRISTENSEN, in J. H. WERNER AND H. P. STRUNK, eds., *Polycrystalline Semiconductors II*, Springer-Verlag, Heidelberg, 1991, p. 145.

4.5 Optical Constants of Cu(In,Ga)Se₂ Thin Films

Author: K. ORGASSA

In collaboration with: U. Rau, H. W. Schock, J. H. Werner

The propagation of light through any homogeneous material is defined by its complex refractive index $\tilde{n} = n - ik$, where the refractive index n and the extinction coefficient k are called *optical constants*. In particular, these properties determine the optical reflectance at the boundaries of the material and the light absorption within the bulk. For a photovoltaic material, optical reflectance and absorptance are the cornerstones for optical losses and photo-generation, and, therefore, establish the link between optical properties and photo-response of a solar cell. For the semiconductor Cu(In,Ga)Se₂ (CIGS), only few data on optical constants are yet available [1,2,3].

In order to obtain optical constants that are well suited for modeling the optical properties of CIGS solar cells, we use the common approach to evaluate the optical constants from measurements of the normal incidence transmittance T_m and reflectance R_m of optically smooth thin CIGS films on glass. This determination method relates closely to (i) the absorber material present in the solar cell, and (ii) to the illumination geometry used for solar cell characterization. The corresponding model system of a stack of plane-parallel flat layers with abrupt interfaces on which a plane wave is incident along the surface normal allows the formulation of analytical expressions for the optical transmittance $T_{an}(n_f, k_f, d_f, n_s)$ and reflectance $R_{an}(n_f, k_f, d_f, n_s)$ in terms of the optical constants of the thin film, n_f and k_f , the film thickness d_f , and the refractive index of the transparent substrate n_s . If film thickness d_f and refractive index n_s are known, the determination of the optical constants $n_f(\lambda)$ and $k_f(\lambda)$ is achieved by solving the implicit equation system in a point-to-point fit for each single wavelength λ [4].

$$T_{an}(n_f(\lambda), k_f(\lambda)) - T_m(\lambda) = 0 \quad (1)$$

$$R_{an}(n_f(\lambda), k_f(\lambda)) - R_m(\lambda) = 0 \quad (2)$$

We prepare samples of Cu(In_{1-x}Ga_x)Se₂ thin films with five representative In/Ga ratios varying from pure CulnSe₂ to pure CuGaSe₂ ($x = 0 \dots 1$). A computer routine serves for the computation of the optical constants n_f and k_f . For a given wavelength λ , this routine solves each of the implicit equations, Eqs. (1) and (2), individually in a defined area of the (n, k) -plane and then looks for intersections of the solutions of either equation. Plotted over λ , the multiple solutions for n_f and k_f form several

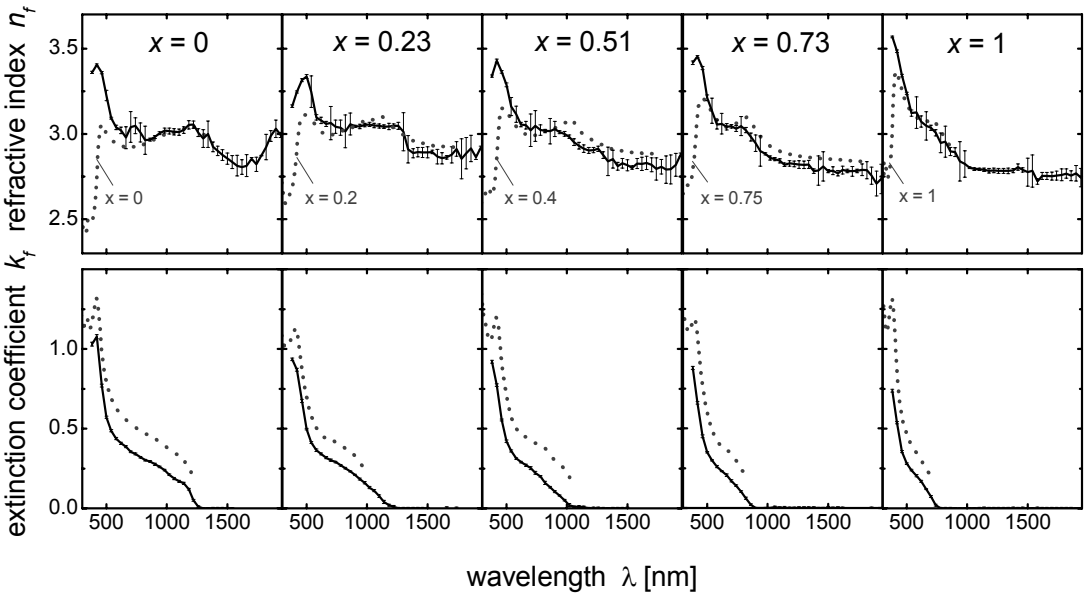


Figure 1: Optical constants of $\text{Cu}(\text{In}_{1-x}\text{Ga}_x)\text{Se}_2$ with relative Ga-contents x as indicated. Solid lines present thin film data of this contribution [4], dotted lines recent data of bulk material [1,2]. The extinction coefficient k_f is significantly lower than that evaluated by spectral ellipsometry of bulk data.

solution branches. The extraction of the true n_f and k_f dispersion curves necessitates an interpretation of these branches in terms of physically meaningful and implausible solutions. However, owing to the existing knowledge of the optical properties of CIGS (see [2] and references therein), the identification of the correct dispersion curve for $n_f(\lambda)$ - and subsequently for $k_f(\lambda)$ - proves to be unproblematic.

Figure 1 presents the optical constants of $\text{Cu}(\text{In}_{1-x}\text{Ga}_x)\text{Se}_2$ thin films on glass (solid lines) with relative Ga-contents x as indicated [4]. The error bars for n_f and k_f indicate the sensitivity of the determination method to the uncertainty Δd_f in the input parameter film thickness. The dotted lines present recent data evaluated from bulk material [1,2].

References:

- [1] M. I. ALONSO, K. WAKITA, J. PASCUAL, M. GARRIGA, AND N. YAMAMOTO, Phys. Rev. B **63**, 075203 (2001)
- [2] M. I. ALONSO, M. GARRIGA, C. A. DURANTE RINCÓN, E. HERNÁNDEZ, AND M. LEÓN, Appl. Phys. A **74**, 659 (2002).
- [3] P. D. PAULSON, R. W. BIRKMIRE, AND W. N. SHAFARMAN, J. Appl. Phys. **94**, 879 (2003).
- [4] K. ORGASSA, U. RAU, H.-W. SCHOCK, AND J. H. WERNER, to be published in Proc. 3rd World Conf Photovolt. Solar Energy Conversion (Osaka, Japan 2003).

4. 6 Qualitative and Quantitative Analysis of Granular CuInSe₂ by Electron Beam Induced Current

Author: GERDA C. GLÄSER

In collaboration with: U. Rau, H.-W. Schock

Monograin-CuInSe₂-solar cells consist of a thick layer of grains embedded in a polymer [1]. The grains with a diameter of about 50μm crystallise from a liquid phase. One of the major problems in measuring and characterising these cells is their heterogeneous nature. Integral measurements are difficult to discuss because of unknown optical and electrical cell properties. Spatially resolving techniques would be most suitable for the investigation of the absorber. One of those techniques is the measurement of electron beam induced currents (EBIC). Micrographs of the EBIC current reveal different response of grains and inhomogeneities within a grain. This is of particular interest because the grains have to be considered as single crystal cells.

We measure the induced currents at different beam energies E_b with a pico-amperemeter. Figure 1 schematically displays the interaction of the cell with the electron beam. The electrical quantum efficiency (QE) is given by

$$QE = \frac{I_{EBIC} \cdot \xi E_g}{(1-f) \cdot I_{Beam} \cdot E_{Beam}} \quad (1)$$

where I_{beam} is the beam current, E_{beam} the beam energy and I_{EBIC} is the measured device current. The product $\xi^* E_g$ describes the amount of energy which is dissipated from the primary electron energy in order to create one electron-hole pair, f is the fraction of backscattered electrons. The effective generation depth R_g of charge carriers in the absorber increases with varying beam energies. If the generation depth R_g exceeds the diffusion length L_d , QE decreases because less charge carriers are collected. The dotted lines of figure 2 represent the measured quantum efficiencies QE of the grains with different activities.

The EBIC- quantum efficiency can also be calculated with

$$QE(E_b) = \int_0^\infty \varphi(z) \cdot g(z, E_b) dz \quad (2)$$

where $\varphi(z)$ denotes the collection probability depending only on electronic properties of the semiconductor [3] and $g(z, E_b)$ is the generation function [2].

Due to the grain diameter of $50 \mu\text{m}$, the generation volume does not interact with the back contact. Hence, we neglect back surface recombination. Therefore it is possible to fit QE with $\varphi(z)$ according to

$$\varphi(z) = e^{-(x-w)/L_d} \quad (3)$$

only considering the width of the space charge region w in the absorber and the diffusion length L_d . In the window region $\varphi(z)$ vanishes, whereas in the space charge region the collection probability approaches unity.

We measure grains that vary in activity on the same sample. As expected, grains that appear brighter in the EBIC-picture have higher electron quantum efficiency QE . Within the above made assumptions, the fits for $\varphi(z)$ yield diffusion lengths between $0.3 \mu\text{m}$ and $0.8 \mu\text{m}$ depending on the activity of the grains.

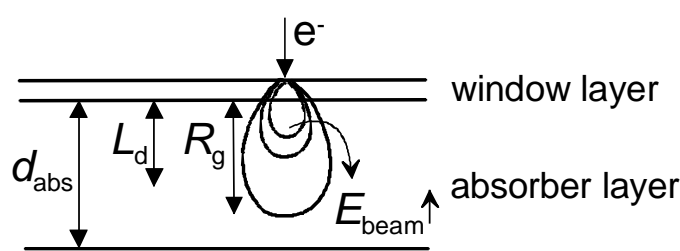


Figure 1: Schematic diagram of the electron beam and the generation volume. The volume varies with changing beam energies E_{beam} but does not interact with the back contact due to the absorber thickness d_{abs} .

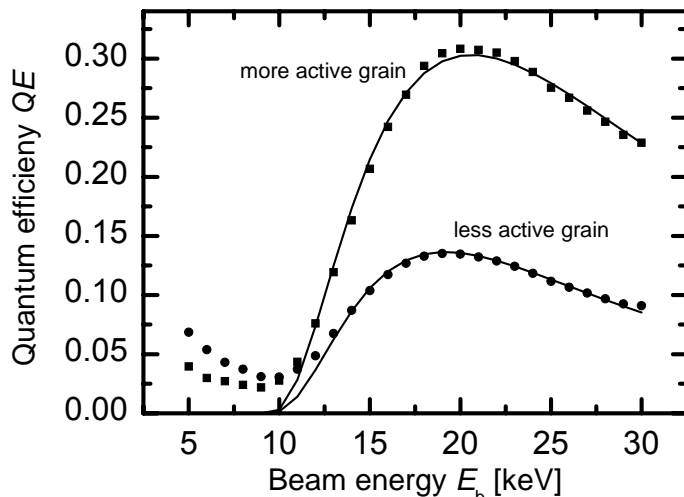


Figure 2: The square and circle dots represent the measured quantum efficiencies QE of the grains of different activities. The solid lines show the fit results. The fit results in diffusion lengths L_d of $0.63 \mu\text{m}$ and $0.34 \mu\text{m}$ respectively. The brighter grain has a higher quantum efficiency QE and diffusion length L_d .

References:

- [1] M. ALTOSAAR, A. JAGOMÄGI, M. KAUK, M. KRUNKS, J. KRUSTOK, E. MELLIKOV, J. RAUDOJ, T. VAREMA, Thin Solid Films **431-432**, 466 (2003).
- [2] T. E. EVERHART, P. H. HOFF, J. Appl. Phys, **42**, 5837 (1971).
- [3] R. R. SCHEER, M. WILHELM, H.J. LEWERENZ, H. W. SCHOCK, L. STOLT, Solar Energy Mater. Solar Cells, **49**, 299 (1997).

4.7 Mechanical Properties of Flexible Cu(In,Ga)Se₂ Solar Cells

Author: P.O. GRABITZ

In Collaboration with G. Bilger, S. Enders¹

The production of flexible, light-weight solar cells on thin and flexible substrates is one of the future challenges in thin-film solar cell technology. The question is if common solar cell materials, e.g. Cu(In,Ga)Se₂ (CIGSe), tolerate the mechanical strain of bending which occurs during preparation and application.

For different bending radii, current voltage (IV)- and quantum efficiency (QE)-measurements were performed. Scanning electron microscope (SEM) and electron beam induced current (EBIC) measurements explain why the efficiencies of convex-bent, i.e. tensile-strained, thin-film solar cells decrease. Figure 1 shows mechanical strain at the bent surface of a flexible substrate. The thicker the substrate, the higher the strain at a given bending radius is. To determine the stress in CIGSe resulting from bending, it is necessary to know Young's modulus E . For CIGSe this constant was measured with a Nanoindenter (SA2 by MTS). In this technique, a little pyramid is pushed on the thin film material until a depth of 500 nm is reached. The depth and the necessary force are measured. With respect to the pyramid geometry it is possible to calculate Young's modulus. Assuming that material of thickness d and length l is bent circularly with a radius r , the maximum relative strain ε in the outermost layer is given by

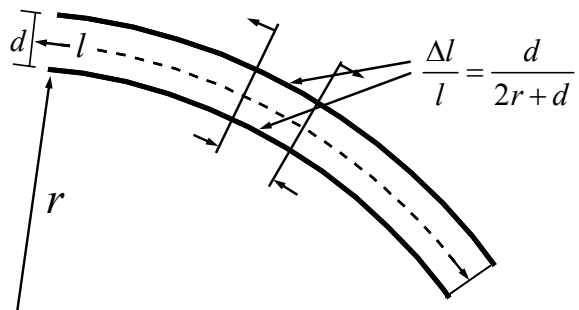


Figure 1: A bent piece of material is stretched on the convex side and pressed on the concave side. In the centre, there is a neutral phase, where no mechanical change occurs during bending. The intensity of strain induced by stretching and pressing is proportional to the thickness of the material and reciprocally proportional to two times the bending radius plus the thickness.

For different bending radii, current voltage (IV)- and quantum efficiency (QE)-measurements were performed. Scanning electron microscope (SEM) and electron beam induced current (EBIC) measurements explain why the efficiencies of convex-bent, i.e. tensile-strained, thin-film solar cells decrease. Figure 1 shows mechanical strain at the bent surface of a flexible substrate. The thicker the substrate, the higher the strain at a given bending radius is. To determine the stress in CIGSe resulting from bending, it is necessary to know Young's modulus E . For CIGSe this constant was measured with a Nanoindenter (SA2 by MTS). In this technique, a little pyramid is pushed on the thin film material until a depth of 500 nm is reached. The depth and the necessary force are measured. With respect to the pyramid geometry it is possible to calculate Young's modulus. Assuming that material of thickness d and length l is bent circularly with a radius r , the maximum relative strain ε in the outermost layer is given by

$$\varepsilon = \frac{\Delta l}{l} = \frac{d}{2r+d}. \quad (1)$$

¹ Max-Planck-Institut für Metallforschung Stuttgart

The correlation between strain ε and stress σ is given by Hook's law: $\varepsilon = E^{-1} \sigma$. For the measured IV- and QE-curves it is now possible to specify stress instead of different bending radii. The experiments yield the following results:

- i. Young's modulus of CIGSe is measured to be $E = 70 \pm 17 \text{ GPa}$. This was the first measurement on a CIGSe thin-film material.
- ii. In the case of a 5 μm CIGSe layer evaporated on a 200 μm thick metal foil, a bending radius of 25 mm results in $\varepsilon = 0.4\%$.
- iii. Compressive stresses up to 0.3 GPa , which accords to $\varepsilon = 0.4\%$, cause no significant effects in I/V- and QE-measurements. Further bending causes blistering of the CIGSe layer.
- iv. At a tensile strain of $\varepsilon = 0.4\%$ the measured efficiency decreases significantly (Fig. 2). Cracks, determined by SEM, are correlated to areas, where no EBIC-signal is found (Fig. 3). It is probably not the CIGSe absorber that deteriorates, but the ZnO window layer.

In the case of cells on 200 μm thick metal foil, a bending radius of 25 mm causes a strain of 0.4 %. Minor bending radii without deterioration of the cell performance may only be reached, if the cells are covered with a transparent layer with mechanical properties equivalent to the substrate.

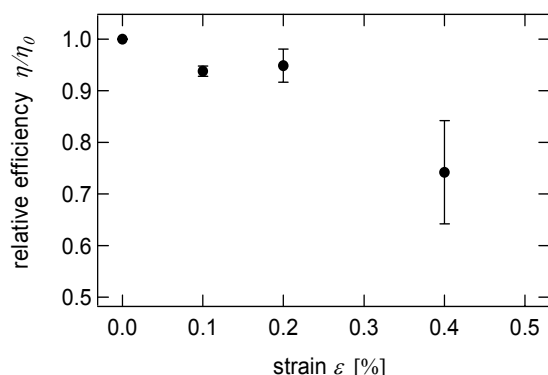


Figure 3: The efficiency of the solar cell relative to the unbent case plotted against the strain caused by convex bending.

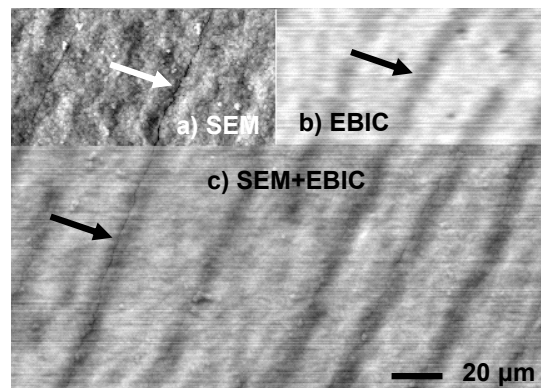


Figure 4: SEM and EBIC pictures of a cell bent to $\varepsilon = 0.4\%$. a) shows the pure SEM image, b) shows EBIC data. Part c), combines SEM and EBIC images. The cracks visible in the SEM correlate to electrically inactive (dark) areas in the EBIC data, as indicated by the arrows

References:

- [1] P.O. GRABITZ, G. BILGER, unpublished.

4.8 Copper-Indium-Gallium-Diselenide/Molybdenum Layers Analyzed by corrected SIMS Depth Profiles

Author: G. BILGER

In collaboration with: A. Strohm, P. O. Grabitz

Polycrystalline Cu(In,Ga)Se₂ (CIGS) acts as a photovoltaic absorber material in thin film solar cells. The absorber layers are grown on molybdenum back contacts deposited on glass or flexible substrates such as metal foils or polymers. During the preparation process, substrate elements diffuse across the back contact into the CIGS. We investigate the diffusion into the CIGS/Mo layers by SIMS depth profiling corrected with respect to recoil mixing and atomic mixing. Detaching the CIGS/Mo layers from the substrate allows profiling the layers from surface-side and backside. Thereby, the intermixing effects caused by the sputtering process for depth profiling can be separated [1].

Comparing the surface-side with the mirrored backside depth profile (Fig. 1) enables us to correct the distortion by recoil mixing (dotted curve). Recoil mixing is anisotropic and different for each element; it primarily depends on the mass relation between the colliding atoms, given by the energy transfer function

$$\gamma = 4m_1m_2/(m_1+m_2)^2. \quad (1)$$

Here, m_1 is the mass of the primary incoming atom (ion) and m_2 the mass of the recoiling target atom. The colliding atoms are an ensemble of all atoms involved in the sputtering event before the emission of an atom or molecule from the surface.

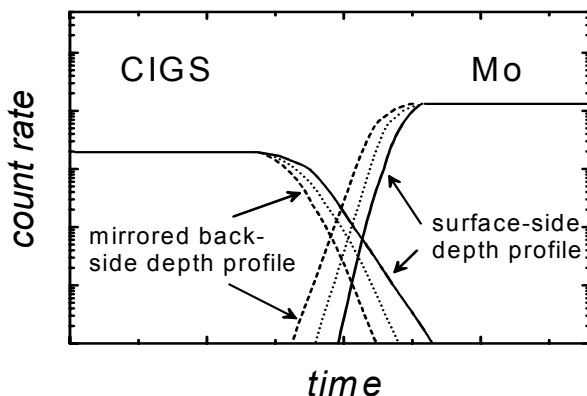


Figure 1: Schematic presentation of the element-specific correction step of recoil mixing. The distorted profiles (solid and dashed lines) are corrected by evaluating the mean time value in the depth profiles from either side of the interface at a given concentration (dotted line).

The remaining recoil-mixing-corrected profile is now only distorted by atomic mixing, which is isotropic for all elements and nearly independent of the matrix. Therefore, a correction function once found for a given element can be applied to all other elements of interest. In order to find that correction function it is necessary to have at least one element whose step function at the interface is known to undergo no diffusion or intermixing during preparation. At the absorber/Mo interface, Mo is the only element which can be regarded as having the benefit of an abrupt interface change in the present scale dimensions. The difference between the real step and the measured profile is the distortion generated by atomic mixing. From the deviation of the real step function we deduce a complementary error function (erfc) -type correction function which is applied to the concentration profiles of the other elements.

Finally, the corrected depth profile allows for the determination of diffusion coefficients of impurities in the complex multinary compound system CIGS. We demonstrate exemplarily the correction procedure for Ga in Fig. 2.

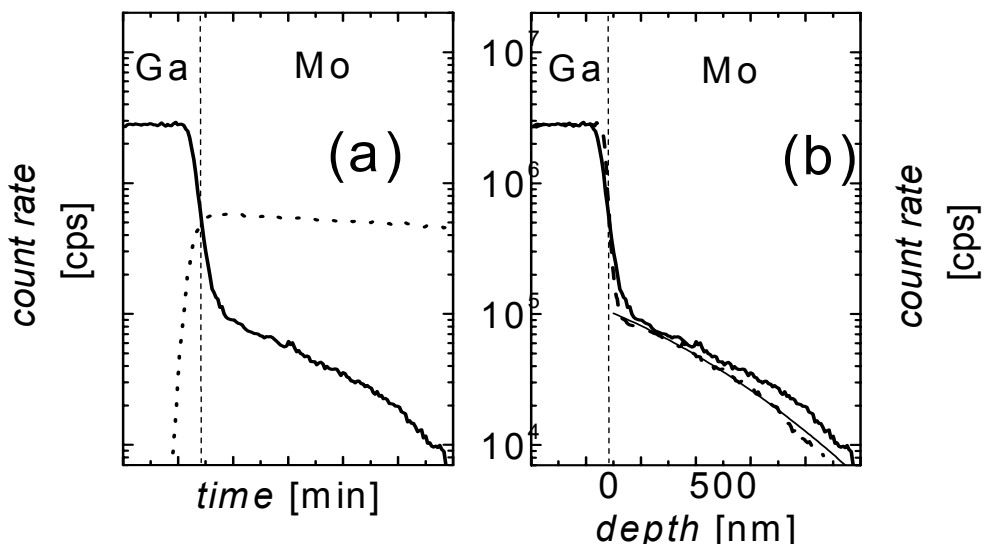


Figure 2: Mo and Ga SIMS profiles after recoil- (a) and atomic-mixing (b) correction. Dotted line: Mo profile after recoil-mixing correction; thick solid lines: Ga profile after recoil-mixing correction; dashed line: Ga profile after atomic-mixing correction; thin solid line: fit of an appropriate solution of the diffusion equation to the Ga diffusion profile. From this fit a diffusion coefficient $D = 5 \times 10^{-17} \text{ m}^2 \text{s}^{-1}$ is extracted.

References:

- [1] G. BILGER, P.O. GRABITZ, A. STROHM, unpublished.

4.9 Laser-Doping of n^+ -Type Silicon Solar Cell Emitters

Author: A. Esturo-Breton

In collaboration with: J. R. Köhler, J. H. Werner

Low-temperature processing of monocrystalline or polycrystalline silicon solar cells has the potential to avoid the production costs of state of the art high-temperature solar cell processing. Such methods do not require expensive equipment and may be competitive, if the throughput can be scaled to a range high enough for in-line processing.

We investigate a pulsed-laser-based doping technique for monocrystalline silicon wafers. Spin-coating of a phosphor-containing doping liquid results in a thin doping layer at the surface of silicon wafers. The focus of a 25 ns pulsed 532 nm frequency doubled Nd:YVO₄-laser melts a thin up to 400 nm thick layer of silicon. Phosphor atoms from the doping layer mix with the liquid silicon. Rapid cooling of the melt after the laser pulse induces epitaxial growth of the solidifying phosphorous-doped silicon on the surface of the p-type crystalline silicon wafer.

By this method we produce p-n junctions with highly n-doped emitters. Figure 1 shows the square resistance of the emitter. The strong decrease of the emitter resistance with increasing laser fluence indicates the existence of a threshold value. This threshold value results from heating up the silicon surface up to melting temperature. If the laser energy further increases, melting of the silicon layer begins. The depth of the melted silicon layer is proportional to a further increase of the laser pulse energy. Therefore, the thickness of the phosphorous-doped layer increases with laser pulse energy density, whereas the measured doping concentration is nearly independent of the pulse energy density. The result is, that the square resistance of the emitter is inversely proportional to the lasers pulse energy density. Figure 1 shows the theoretical values of the square resistance fitted to the experimental results.

We use this doping process for the production of 4 cm²-sized solar cells. Figure 2 shows the current/voltage characteristics of a solar cell. We process the emitter on a 375 μm thick boron doped FZ-wafer with a resistivity of $\rho = 0.35 \Omega\text{cm}$ using a laser power of 0.4 W. The cell has an open circuit voltage $V_{oc} = 619 \text{ mV}$, a short circuit current density $J_{sc} = 33.9 \text{ mA/cm}^2$ and an efficiency $\eta = 15.6 \%$.

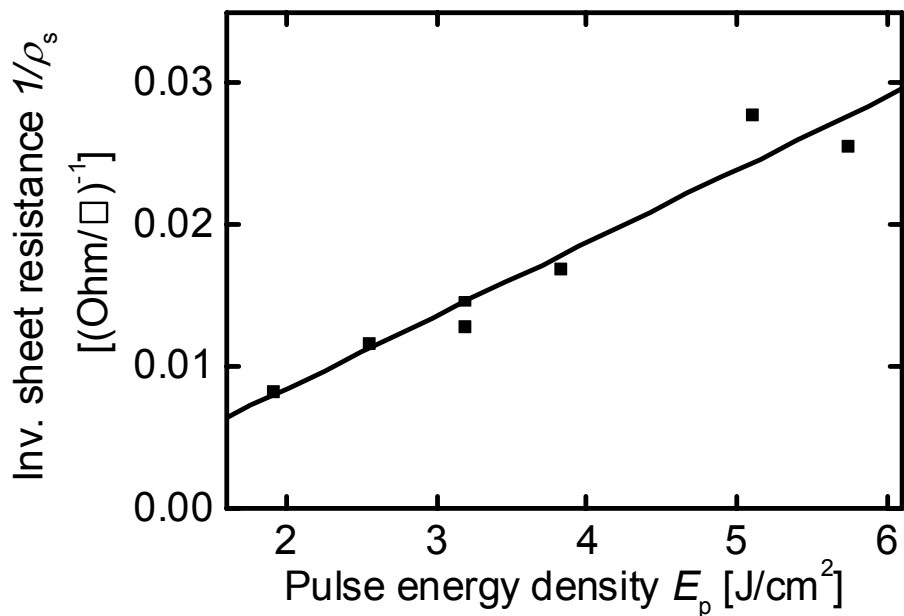


Figure 1: The square resistance ρ_s of laser-doped emitters decrease inversely proportional to the pulse energy density E_p according to $\rho_s^{-1} = C(E_p - E_{th})$, with a threshold energy density $E_{th} = 0.36 \text{ J/cm}^2$ and $C = 5.2 \times 10^3 \text{ } (\Omega/\square)^{-1}/(\text{J/cm}^2)$. Theoretical values (solid line) are fitted to experimental results (solid symbols).

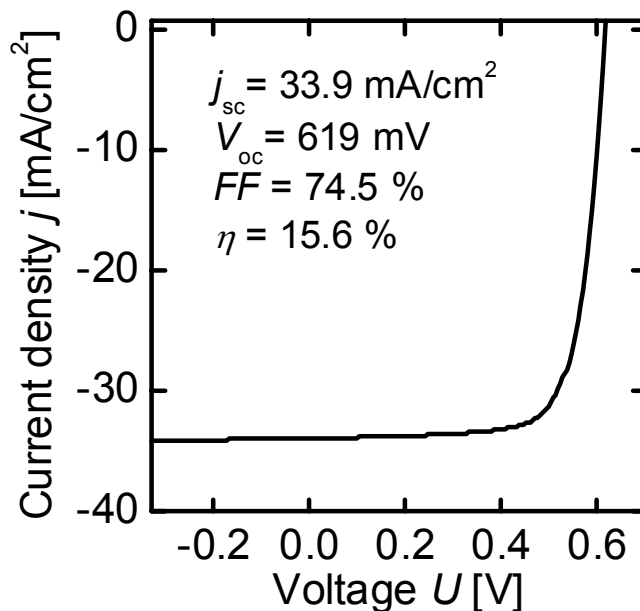


Figure 2: Current/voltage characteristics of a $2 \times 2 \text{ cm}^2$ solar cell with laser-doped n^+ -emitter.

4.10 Monocrystalline Transfer Silicon with 150 mm Diameter

Author: C. BERGE

In collaboration with: M. Zhu, M. Schubert, J. H. Werner

The transfer of monocrystalline silicon layers as a way for fabricating thin-film monocrystalline silicon on foreign substrates is one of the key research topics in the silicon group. Last year, we reported the successful transfer of such films onto flexible substrates, resulting in a 14.6 % efficient flexible silicon solar cell [1,2], and we still hold the efficiency record for silicon thin-film solar cells [3].

Our transfer process comprises the electrochemical formation of a porous double layer on a silicon substrate, subsequent epitaxial deposition of the silicon device layer on top of the porous substrate surface, device processing by standard wafer technology, and the final transfer of the device layer using the porous layer structure as a "zipper" to detach it from the host wafer.

In 2003, we successfully extended the process from 100 mm wafer technology to 150 mm technology. To enable this upscaling, we developed a new etching system for the formation of the starting porous layer. Figure 1 shows a photograph of this new setup. Apart from the increased substrate size, the system features two more major improvements. The liquid handling is completely automated and microprocessor-controlled, which reduces contamination risk of the etching solution and provides easier handling, and the substrate is fixed inside the system on a vacuum chuck. The latter feature allows complete exposure of the wafer front side to the etching solution, thus the complete front side of the substrate wafer is etched, and enables the transfer of silicon sheets with the complete diameter of 150 mm.

To improve the lateral homogeneity of the porous layers, we performed extensive simulations of the etching current distribution inside the cell using finite element modeling (FEM). Figure 2 shows a calculated two-dimensional potential and current density distribution inside the cell during etching. The numerical simulations correlate well with observations from our experiments and indicate further routes to improve and control the quality of the transfer process.

As one of the aims of our process is the fabrication of flexible solar cells, we investigated the mechanical properties of 25 µm thin silicon sheets that we obtained from our transfer process. Preliminary studies prove that unsupported free standing films can be bent to a minimum

curvature radius of approximately 2 mm without breaking [4]. These minimum curvatures seem sufficient for integrating solar cells into curved surfaces of small consumer electronics like CD players, mobile phones, and a wide range of typical office tools.

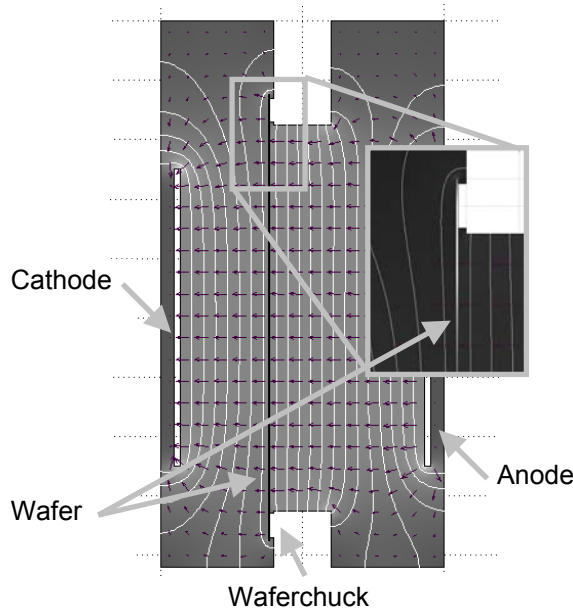


Figure 1: FEM-Simulation of potential (contours) and current density (surface colors) in the etching cell. The black arrows indicate the direction of the current flow. The blow-up shows a more detailed view of the potential and current density within the thin silicon wafer close to the wafer mount.

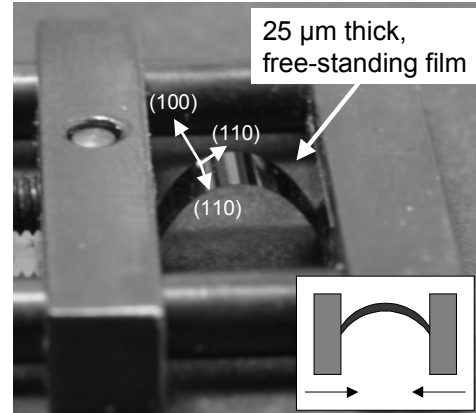


Figure 2: The photograph shows a free-standing, uncoated 25 μm thick silicon film of $8 \times 3 \text{ mm}^2$, placed between the two plates of a micro bench vice. Reducing the distance between the two plates leads to parabolic bending of the thin film as indicated in the small schematic, and allows experimental estimation of the minimum curvature radius.

References:

- [1] R. B. BERGMANN, C. BERGE, T. J. RINKE, J. SCHMIDT, AND J. H. WERNER, Sol. En. Mat. & Solar Cells **74**, 213 (2002).
- [2] J. H. WERNER, T. A. WAGNER, C. GEMMER, C. BERGE, W. BRENDLE, AND M. B. SCHUBERT, in *Proc. 3rd World Conference on Photovoltaic Solar Energy Conversion* (2003), in print.
- [3] M. A. GREEN, K. EMERY, D. L. KING, S. IGARI, AND W. WARTA, Progress in Photovoltaics: Res. & Appl. **10**, 55 (2002).
- [4] C. BERGE, T. A. WAGNER, W. BRENDLE, C. CRAFF CASTILLO, M. B. SCHUBERT, AND J. H. WERNER, Mat. Res. Soc. Symp. Proc. **769**, H2.7.1 (2003).

4.11 Recent Developments in Integrated Photovoltaics

Author: M. SCHUBERT

In collaboration with: C. Gemmer, C. Wagner, J. Krämer, J. H. Werner

Solar cells not only serve for generating electricity at a kW-level on rooftops, but they also enable the mobile use of modern electronic appliances with no need for charging batteries, or carrying heavy and bulky mains-connecting power supplies.

Under the label "integrated photovoltaics - *ipv*", *ipe* develops solar cells and small prototype systems for illustrating the potential of such mobile photovoltaic (PV) power supply. One of the prerequisites for such endeavours is to precisely know how much energy the electronic devices (like CD or MP3 players, mobile phones etc.) need, and how much energy they can get from a PV system in practical use. Investigating the performance of different types of solar cells under varying illumination spectra, intensities etc., C. Gemmer gives detailed guidelines for designing *ipv* systems [1].

More practically, after our first solar jackets [2] presented in Fig. 1, we now develop advanced charge control electronics for making best use of varying illumination conditions in *ipv*-systems. Similar to module-integrated inverters in rooftop- or facade-integrated PV systems, every series-connected string of solar cells in an *ipv* jacket, sportswear, or backpack now delivers its electrical power to the storage battery via an individual charge controller. One of such string converters of 22x17 mm² size powers the wireless PV keyboard of Fig. 2, constructed by C. Wagner during his Studienarbeit [3]. For future *ipv*-systems, a novel string controller design greatly enhances the charge storage efficiency under low light conditions, and at the same time shrinks the controller size to 12x12 mm² [4].

For bringing clothing-integrated photovoltaics closer to the market, the local state of Baden-Württemberg started funding of the SOLARTEX programme in March 2003. In cooperation with several garment and textile companies, as well as with two research institutes, we are tailoring *ipv* applications and are addressing issues like the integration of solar cells into clothes, their electrical connection, durability, washing of respective garments etc.

The accompanying development of flexible solar cells at *ipe* comprises two different technologies: amorphous and thin monocrystalline silicon. With flexible monocrystalline transfer cells (cf. chapter

4.10 of this report), we so far reach conversion efficiencies up to 14.6% [2]. Unless very low light levels below 1000 Lux are targeted, the almost ideal logarithmic intensity dependence of crystalline silicon outperforms the efficiency of amorphous silicon cells which suffer from lower efficiency at full solar illumination as well as from an intensity dependence controlled by a diode quality factor close to two. On the other hand, only amorphous cells of 0.5 micron thickness offer superior and almost textile flexibility.



Figure 1: Demonstration of garment integrated photovoltaics. These first prototypes use rigid high-performance crystalline silicon cells, and one single charge controller for all strings connected in parallel.

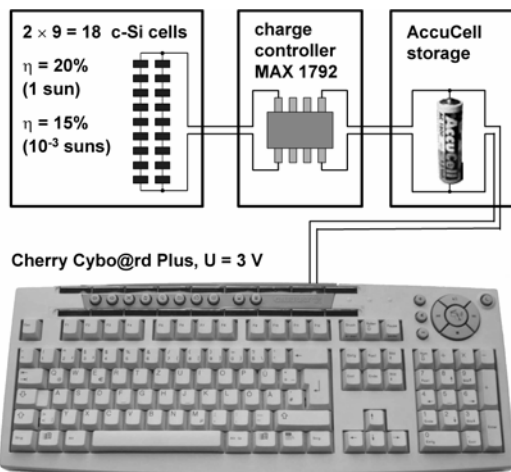


Figure 2: The photovoltaic power supply of our wireless keyboard proves its benefits in everyday use at the ipe library. A similar commercial product became available just recently [5].

References:

- [1] C. GEMMER, Analytische und numerische Untersuchungen von Solarzellen unter wechselnden Beleuchtungsbedingungen, Dissertation, Universität Stuttgart, Institut für Physikalische Elektronik (2003).
- [2] J. H. WERNER, T. A. WAGNER, C. GEMMER, C. BERGE, W. BRENDLE, AND M. B. SCHUBERT, Recent progress on transfer-Si solar cells at *ipe* Stuttgart, in *Proc. 3rd World Conference on Photovoltaic Solar Energy Conversion* (2003), in print.
- [3] C. WAGNER, Photovoltaikversorgung von Computer-Eingabegeräten, Studienarbeit, Universität Stuttgart, Institut für Physikalische Elektronik (2003).
- [4] J. KRÄMER, Autonome Solarstrom-Versorgung elektronischer Kleingeräte in Ski-Bekleidung, Studienarbeit, Universität Stuttgart, Institut für Physikalische Elektronik (2003).
- [5] <http://www.cherrycorp.com>

4.12 Closed-Form Expression for the Current/Voltage Characteristics of pin Solar Cells

Author: K. TARETTO

In collaboration with: U. Rau, J. H. Werner.

A *pin*-structure comprises an intrinsic layer sandwiched between two highly doped p- and n-type layers. This type of structure is the standard in a-Si solar cells, and since a few years it is successfully utilized for high-efficiency microcrystalline Si [1] and nanocrystalline Si [2] solar cells. Despite its wide-spread use, there was up to now no simple closed-form equation for the current (J)/ voltage (V) characteristics of *pin*-junctions.

This work [3] presents a new model for the J/V -equation in pin diodes and *pin*-solar cells. By solving the continuity equations considering drift and diffusion, we obtain a general analytical expression for the J/V -characteristics. The main physical simplifications assumed within our model are:

- (i) the electric field in the intrinsic layer is constant,
- (ii) the current density does not exceed a critical value, which in most practical cases is sufficiently high,
- (iii) the photogeneration rate is homogeneous within the i-layer,
- (iv) the carrier mobilities μ and lifetimes have the same values for electrons and holes.

Assumptions (i) to (iv) enable to find simple analytical expressions for the current/voltage equation of the *pin*-solar cell, considering both drift and diffusion currents [3]. Figure 1 shows that the inclusion of both types of currents results in voltage-dependent diode ideality factors n_{id} . At high diffusion lengths L , n_{id} ranges from 1.8 at low to 1.2 at high applied voltages, while the value $n_{id} = 1.8$ holds for the whole characteristics at low L .

Figure 2 compares the dark current/voltage characteristics at different temperatures obtained from our model, to experimental current/voltage curves measured in thin-film microcrystalline silicon solar cells, showing that our model accurately explains the output characteristics of *pin* solar cells. The curves in Figure 2 are best fitted using diffusion length of $L = 17 \mu\text{m}$, which explains the high efficiencies achieved by these cells [1].

Regarding the characteristics under illumination, a simple equation for the short-circuit current density is obtained, which shows that the collection efficiency in *p-i-n* solar cells is controlled by both drift and diffusion. We then utilize our model to explain the experimentally found increase of solar cell efficiency with the mobility-lifetime product in nanocrystalline silicon *p-i-n* solar cells [2].

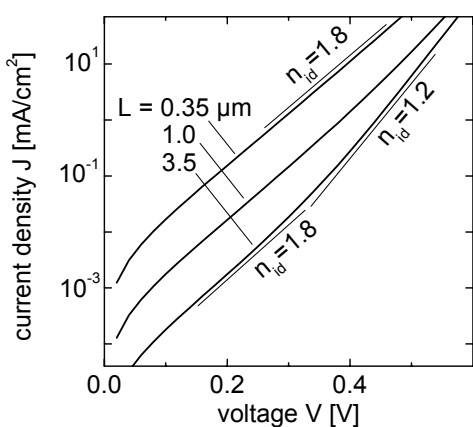
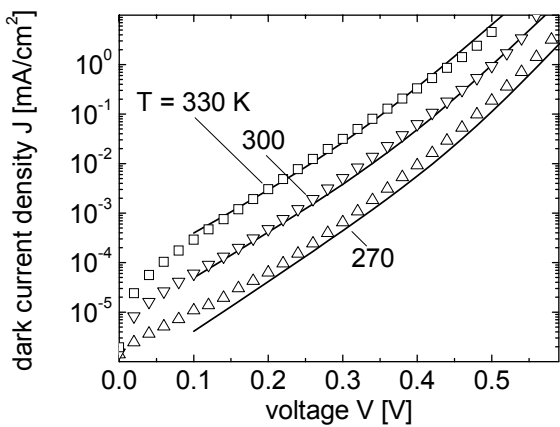


Figure 1: The dark current/ voltage characteristics, show different diode ideality factors n_{id} depending on voltage and diffusion length L . At high diffusion lengths and low voltages, n_{id} takes the value $n_{id} = 1.8$, turning to $n_{id} = 1.2$ at high voltages. At small diffusion lengths, we have $n_{id} = 1.8$ independently of voltage.



*Figure 2: Dark current/ voltage characteristics of nanocrystalline Si *p-i-n* diodes measured at different temperatures (symbols), fitted with our equation (solid lines). These curves are best fitted using diffusion length of $L = 17 \mu\text{m}$, which explains the high efficiencies achieved by these cells [1].*

References:

- [1] K. YAMAMOTO, M. YOSHIMI, Y. TAWADA, Y. OKAMOTO, A. NAKAJIMA, AND S. IGARI, Appl. Phys. A **69**, 179 (1999).
- [2] N. WYRSCH, L. FEITKNECHT, C. DROZ, P. TORRES, A. SHAH, A. PORUBA, AND M. VANECEK, J. Non-Cryst. Solids **266-269**, 1099 (2000).
- [3] K. TARETTO, U. RAU, AND J. H. WERNER, Appl. Phys. A **77**, 865 (2003).

4.13 Influence of the Built-in Voltage on the Fill factor of Dye-Sensitized Solar Cells

Author: G. KRON

In collaboration with: M. Duerr¹, T. Miteva¹, G. Nelles¹, A. Yasuda¹, K. Taretto,
U. Rau, J. H. Werner

Dye-sensitized solar cells (DSSC) [1] are an interesting low-cost alternative to conventional solar cells and, therefore, have attracted considerable interest during the past decade. The basic photovoltaic action of these devices has been studied extensively in the past. After photoexcitation of the dye and ultrafast injection of the excited electrons into the conduction band of the TiO₂, the charge carrier transport occurs by diffusion in the nanoporous TiO₂ network towards the contacting material. An (equilibrium) built-in voltage V_b^0 evolves close to the interface between the nanoporous TiO₂ and the contacting SnO₂:F front electrode. However, the importance of this junction potential V_b^0 for the photovoltaic performance of the DSSC is still controversially discussed.

The present work manipulates V_b^0 in DSSCs by using different front contact materials and by investigating the influence of these contact variations on all photovoltaic parameters, i.e., on the complete illuminated current density (J)/voltage (V) characteristics of the devices. By comparing a theoretical model [2] to our experimental results [3], we find that there is no requirement for a charge-separating field in a photovoltaic device, for what concerns the build-up of an open circuit voltage V_{oc} or for a proper charge collection under short circuit conditions. However, a device that is well performing under operation conditions, i.e., that possesses not only V_{oc} and a short circuit current J_{sc} but also a reasonable fill factor FF , clearly requires a built-in field.

For the preparation of the DSSCs under investigation, we use glass substrates covered with four different conducting materials: the standard SnO₂:F as well as Al, Au, and ZnO:Al. The range of work function embraced by these materials stretches from E_w (Al) ≈ 4.3 eV to E_w (Au) ≈ 5.1 eV. Figure 1 shows the measured J/V-characteristics of the four devices under illumination through the semi-transparent Pt-back electrode. Whereas the standard SnO₂:F contact yields the best efficiency, mainly because of the high fill factor, the front contact materials with higher E_w and, therefore, lower V_{bi}^0 , i.e. ZnO and Au, lead to a degenerate, S-shaped J/V-characteristics. While we observe huge

¹ Sony International (Europe) GmbH, MSL, Stuttgart, Germany

variations of the fill factors between the different devices, the values of V_{oc} differ only slightly (but consistently with E_w), e.g., $V_{oc} = 0.75$ V of the Al-DSSC lies above $V_{oc} = 0.72$ V of the standard device whereas $V_{oc} = 0.7$ V (Au) and $V_{oc} = 0.66$ V (ZnO) for the DSSCs with the higher work functions.

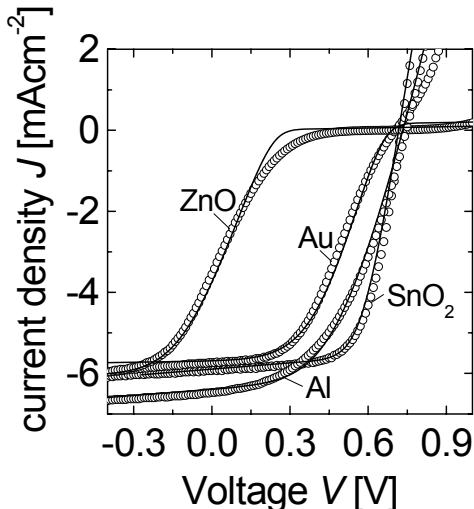


Figure 1: Experimentally measured current density (J)/ voltage (V)-characteristics of the four devices under investigation (open circles). The influence on the fill factor for the DSSCs with higher work functions (Au and ZnO) can clearly be seen. The experimental data are fitted to the analytical model of Ref. [2] (straight lines). The good match between theory and experiment allows us to determine the values for the barrier height Φ_b between the front contact material and the TiO_2 as well as the dark built-in voltages V_b^0 where we find $V_b^0 \geq 0.6$ V ($SnO_2:F$ and Al), $V_b^0 = 0.5$ V (Au), and $V_b^0 = 0.1$ V (ZnO:Al) [3].

Figure 3 also shows the fits (solid lines) of our model [2] to all four measured J/V -characteristics. From these fits we extract the barrier heights Φ_b between the front contact materials and the TiO_2 as well as the dark-built-in voltages V_b^0 with $V_b^0 \geq 0.6$ V ($SnO_2:F$ and Al), $V_b^0 = 0.5$ V (Au), and $V_b^0 = 0.1$ V (ZnO:Al) [3].

We finally conclude that variations of the dark built-in voltage V_b^0 in DSSCs (like in other types of solar cells) primarily affect the fill factor, i.e., the operation of these devices under maximum power conditions. In contrast, the impact of V_b^0 on the generation of a photovoltage, i.e. on V_{oc} , and on carrier collection, i.e. on J_{sc} , if any, is marginal.

References:

- [1] B. O'REGAN AND M. GRAETZEL, Nature **353**, 737 (1991).
- [2] G. Kron, T. Egerter, J. H. Werner, and U. Rau, J. Phys. Chem. B **107**, 3556 (2003).
- [3] G. Kron, *Ladungsträgertransport in farbstoffsensibilisierten Solarzellen auf Basis von nanoporösem TiO_2* , PhD Thesis (Universität Stuttgart, 2003).

5. Verzeichnis der Publikationen/ *List of Publications*

(erschienen 11/2002 bis 10/2003 / published 11/2002 to 10/2003)

- 1 C. BERGE, T. A. WAGNER, W. BRENDLE, C. CRAFF-CASTILLO, M. B. SCHUBERT, AND J. H. WERNER, *Flexible Monocrystalline Si Films for Thin Film Devices from Transfer Processes*, Mat. Res. Soc. Symp. Proc. **769**, H2.7 (2003).
- 2 G. HANNA, J. MATTHEIS, V. Laptev, Y. Yamamoto, U. Rau, and H. W. Schock, *Influence of the Selenium Flux on the Growth Cu(In,Ga)Se₂ Thin Films*, Thin Solid Films **431-432**, 31 (2003).
- 3 M. IGALSON, M. BODEGARD, L. STOLT, AND A. JASENEK, *The 'Defected Layer' and the Mechanism of the Interface-Related Metastable Behavior in the ZnO/CdS/Cu(In,Ga)Se₂ Devices*, Thin Solid Films **431-432**, 153 (2003).
- 4 A. JASENEK, U. RAU, K. WEINERT, H. W. SCHOCK, AND J. H. WERNER, *Illumination-Enhanced Annealing of Electron Irradiated Cu(In,Ga)Se₂ Solar Cells*, in *Proc. 29th IEEE Photov. Spec. Conf.* (IEEE, New York, 2002) p. 872.
- 5 A. JASENEK, U. RAU, K. WEINERT, H. W. SCHOCK, AND J. H. WERNER, *Illumination-Induced Recovery of Cu(In,Ga)Se₂ Solar Cells after High-Energy Electron Irradiation*, Appl. Phys. Lett. **82**, 1410 (2003).
- 6 R. KNIESE, D. HARISKOS, G. VOORWINDEN, U. RAU, AND M. POWALLA, *High Band Gap Cu(In,Ga)Se₂ Solar Cells and Modules Fabricated with in-line Co-evaporation*, Thin Solid Films **431-432**, 543 (2003).
- 7 I. M. KÖTSCHAU, G. BILGER, AND H. W. SCHOCK, *Depth Profiling of Cu(In,Ga)Se₂ by Grazing Incidence X-ray Diffraction*, Mat. Res. Soc. Conf. Proc. **763**, B6.2 (2003).
- 8 I. M. KÖTSCHAU AND H. W. SCHOCK, *Depth profile of the lattice constant of the Cu-poor surface layer in (Cu₂Se)_{1-x}(In₂Se₃)_x evidenced by grazing incidence X-ray diffraction*, J. Phys. Chem. Solids **64**, 1559 (2003).
- 9 G. KRON, U. RAU, M. DÜRR, T. MITEVA, G. NELLES, A. YASUDA, AND J. H. WERNER, *Diffusion Limitations to I₃⁻/I⁻ Electrolyte Transport through Nanoporous TiO₂ Networks*, Electrochim. Solid-State Lett. **6**, E11 (2003).
- 10 G. KRON, T. EGERTER, J. H. WERNER, AND U. RAU, *Electronic Transport in Dye Sensitized Nanocrystalline TiO₂ Solar Cells – Comparison of Electrolyte and Solid-State Devices*, J. Phys. Chem. B **107**, 3556 (2003).
- 11 G. KRON, U. RAU, AND J. H. WERNER, *Influence of the built-in voltage on the fill factor of dye sensitized solar cells*, J. Phys. Chem. B **107**, 13258 (2003).
- 12 M. NERDING, S. CHRISTIANSEN, R. DASSSOW, K. TARETTO, J. R. KOEHLER, AND H. P. STRUNK, *Tailoring Texture in Laser Crystallization of Silicon Thin-Films on Glass*, Solid State Phenomena **93**, 173 (2003).

- 13 Q. NGUYEN, K. ORGASSA, I. M. KÖTSCHAU, U. RAU, AND H. W. SCHOCK, *Influence of Heterointerfaces on the Performance of Cu(In,Ga)Se₂ Solar Cells with CdS and In(OH_xS_y) Buffer Layers*, Thin Solid Films **431-432**, 330 (2003).
- 14 Q. NGUYEN, G. BILGER, U. RAU, AND H. W. SCHOCK, *Modification of Cu(In,Ga)Se₂ Surface by Treatment in Cadmium Solutions*, Mat. Res. Soc. Conf. Proc. **763**, B8.17 (2003).
- 15 K. ORGASSA, H. W. SCHOCK, AND J. H. WERNER, *Alternative Back Contact Materials for Thin Film Cu(In,Ga)Se₂ Solar Cells*, Thin Solid Films **431-432**, 387 (2003).
- 16 N. OTT, G. HANNA, M. ALBRECHT, U. RAU, J. H. WERNER, AND H. P. STRUNK, *Cathodoluminescence Studies of Cu(In,Ga)Se₂ Thin-Films*, Solid State Phenomena **93**, 133 (2003).
- 17 F. PFISTERER, *The Wet-Topotaxial Process of Junction Formation and Surface Treatments of Cu₂S-CdS Thin-Film Solar Cells*, Thin Solid Films **431-432**, 470 (2003).
- 18 U. RAU AND M. TURCU, *Role of Surface Band-gap Widening in Cu(In,Ga)(Se,S)₂ Thin-Films for the Photovoltaic Performance of ZnO/CdS/Cu(In,Ga)(Se,S)₂ Heterojunction Solar Cells*, Mat. Res. Soc. Conf. Proc. **763**, B8.8 (2003).
- 19 U. RAU, G. KRON, AND J. H. WERNER, *Reply to Comments on "Electronic Transport in Dye-Sensitized Nanoporous TiO₂ Solar Cells - Comparison of Electrolyte and Solid-State Devices": On the Photovoltaic Action in pn-Junction and Dye-Sensitized Solar Cells*, J. Phys. Chem. B **107** 13547 (2003).
- 20 B. SCHATTAT, W. BOLSE, S. KLAUMUNZER, F. HARBSMEIER, AND A. JASENEK, *Atomic Mixing of Ni₂O₃/SiO₂, NiO/SiO₂, and Ni/SiO₂ Interfaces Induced by Swift Heavy Ion Irradiation*, Appl. Phys. A **76**, 165 (2003).
- 21 B. SCHATTAT, W. BOLSE, S. KLAUMUNZER, F. HARBSMEIER, AND A. JASENEK, *Interface Mixing of CuO_x/SiO₂ Bilayers by Swift Heavy Ions*, Nucl. Instrum. Meth. B **191**, 577 (2002).
- 22 T. SCHLENKER, H. W. SCHOCK, AND J. H. WERNER, *Initial Growth Behavior of Cu(In,Ga)Se₂ on Molybdenum Substrates*, J. Cryst. Growth **259**, 47 (2003).
- 23 T. SCHLENKER, K. ORGASSA, H. W. SCHOCK, AND J. H. WERNER, *Nucleation of Cu(In,Ga)Se₂ on Molybdenum Substrates*, Mat. Res. Soc. Conf. Proc. **763**, B8.7 (2003).
- 24 H. W. SCHOCK, *Material Related Prerequisites for Chalcopyrite Based Thin Film Solar Cells*, Mat. Res. Soc. Conf. Proc. **763**, B1.6 (2003).
- 25 K. TARETTO, U. RAU, AND J. H. WERNER, *Closed-Form Expression for the Current/Voltage Characteristics of pin Solar Cells*, Appl. Phys. A **77**, 865 (2003).

- 26 K. TARETTO, U. RAU, AND J. H. WERNER, *Method to Extract the Diffusion Length from Solar Cell Parameters – Application to Polycrystalline Silicon*, *J. Appl. Phys.* **93**, 5447 (2003).
- 27 K. TARETTO, U. RAU, T. A. WAGNER, AND J. H. WERNER, *A Simple Method to Extract the Diffusion Length from the Output Parameters of Solar Cells – Application to Polycrystalline Silicon*, *Solid State Phenomena* **93**, 399 (2003).
- 28 M. TURCU AND U. RAU, *Fermi Level Pinning at CdS/Cu(In,Ga)(Se,S)₂ Interfaces: Effect of Chalcopyrite Alloy Composition*, *J. Phys. Chem. Solids* **64**, 1591 (2003).
- 29 M. TURCU AND U. RAU, *Compositional Trends of Defect Energies, Band Alignments, and Recombination Mechanisms in the Cu(In,Ga)(Se,S)₂ Alloy System*, *Thin Solid Films* **431-432**, 158 (2003).
- 30 T. A. WAGNER AND U. RAU, *Temperature Dependent Quantum Efficiency Measurements for the Analysis of Recombination Centers in Epitaxial Silicon Thin-Film Solar Cells*, *Appl. Phys. Lett.* **82**, 2637 (2003).
- 31 T. A. WAGNER, L. OBERBECK, R. B. BERGMANN, M. NERDING, H. P. STRUNK, AND J. H. WERNER, *Low-Temperature Epitaxy on Polycrystalline Silicon Substrates*, *Solid State Phenomena* **93**, 121 (2003).
- 32 K. WEINERT, A. JASENEK, AND U. RAU, *Consequence of 3-MeV Electron Irradiation on the Photovoltaic Output Parameters of Cu(In,Ga)Se₂ Solar Cells*, *Thin Solid Films* **431-432**, 453 (2003).

6 Promotionen 2003 / Ph. D. Theses 2003

GEMMER, CHRISTIAN	Analytische und numerische Untersuchungen von Solarzellen unter wechselnden Beleuchtungsbedingungen
KÖTSCHAU, IMMO	Strukturelle Eigenschaften von Cu(In,Ga)(Se,S) ₂ -Dünnschichten
KRON, GREGOR	Ladungsträgertransport in farbstoffsensibilisierten Solarzellen auf Basis von nanoporösem TiO ₂
RINKE, TITUS	Transfersolarzellen aus monokristallinem Dünnschichtsilicium
ROJAHN, MARTIN	Encapsulation of a retina implant
TARETTO, KURT	Modelling and characterization of polycrystalline silicon for solar cells and microelectronics
WAGNER, THOMAS	Low temperature silicon epitaxy – defects and electronic properties
WEINERT, KRISTIN	Einfluss von Protonen- und Elektronenbestrahlungen auf die photovoltaischen Parameter von Cu(In,Ga)Se ₂ -Solarzellen

Nachtrag / Addendum

DULLWEBER, THORSTEN	Optimierung des Wirkungsgrades von Cu(In,Ga)Se ₂ -Solarzellen mittels variablem Verlauf der Bandlücke, 2002
JENSEN, NILS	Heterostruktursolarzellen aus amorphem und kristallinem Silicium, 2002

7 Diplomarbeiten 2003 / Diploma Thesis Projects 2003

BOZSA, ANDREAS	Nanokristalline Si-Solarzellen aus gepulster Gasphasenabscheidung
ESTURO-BRETÓN, AINHOA	Emitterdiffusion für Silicium-Solarzellen mittels Laserannealing
LUÍS, MARTA	Einfluss der Nukleationsphase auf das Wachstum dünner Cu(In,Ga)Se ₂ -Schichten
NYANOD, NDONGWA	Aufnahme und Wiedergabe großformatiger Bilder
ROSTAN, JOHANNES	Sammlungseigenschaften von Cu(In,Ga)Se ₂ - Solarzellen mit transparenten Rückkontakten
SCHLEUßNER, SEBASTIAN	Optical trapping for CIGS thin film solar cells – Preparation and characterization of test devices
SPEER, TIM	Wechselrichter für Photovoltaik-Systeme

8 Studienarbeiten 2003 / Major Term Projects 2003

BOGICEVIC, MARTIN	Ortsaufgelöste Charakterisierung von Monograin-Solarzellen
BOZSA, ANDREAS	Inbetriebnahme eines automatischen Inspektionsplatzes und die Erstellung von Inspektionsstrategien
GAUGLER, ELMAR	Entwurf von Power-on Reset Schaltungen für die neue 0.5 µm CMOS Mixed-Signal Gate Array Umgebung am IMS
KERN, ALBRECHT	Messung der zeitlichen Helligkeitsverteilung einer Versuchs-OLED
MADER, DENIS	Quasi-epitaktisches Wachstum von Cu(In,Ga)Se ₂ – Schichten auf laserkristallisierten Saatschichten
STAACK, JOCHEN	Untersuchung optischer Eigenschaften farbstoffsensibilisierter Solarzellen
WAGNER, CHRISTOF	Photovoltaik-Versorgung von Computer-Eingabegeräten
WERNER, JÖRG	Programmierung einer grafischen Bedienoberfläche für die Steuerung einer Vakuum-Beschichtungsanlage mit Visual Basic
ZINßER, BASTIAN	Solare Stromerzeugung auf Zypern – Erfassen und Aufbereiten von Daten

9 ipe Kolloquium 2003

- 13.01. BERNHARD DIMMLER, Würth Solar GmbH & Co.KG, „*CIS-Solarmodule, Pilotfertigung bei Würth Solar*“
- 20.01. WOLFGANG WEIMER-JEHLE, Akademie für Technikfolgenabschätzung Baden-Württemberg, „*Zwischen Visionen und Restriktionen – Technikfolgenabschätzung im Problemfeld Energie*“
- 28.04. FRITZ H. KLOTZ, ZSW Stuttgart, „*Thermohydraulische Solarnachführung – Einsatz in Freilandanlagen und an Gebäuden*“
- 5.05. ULRICH GRÄBER, IER, Univ. Stuttgart, und ZES, Stuttgart, „*Konzeption und Entwicklung von dezentralen Versorgungsstrukturen*“
- 12.05. CHRISTOF NEBEL, Walter-Schottky-Institut, TU München, „*Thin-film silicon and Si-Ge alloys for photovoltaic applications*“
- 26.05. LUISA DE COLA, IMC, Molecular Photonics Group, Universiteit van Amsterdam, „*Electroluminescent devices*“
- 2.06. STEFAN GLUNZ, FhG-ISE, Freiburg, „*Lebensdauerspektroskopie zur Analyse von Defekten in Silicium*“
- 23.06. GERHARD STROBL, RWE Solutions, Heilbronn, „*Solarzellen für die Weltraumfahrt*“
- 30.06. HEINZ SCHWEIZER, 4. Physikalisches Institut, Universität Stuttgart, „*DFB- und DBR-Laser im nitridischen Materialsystem*“
- 7.07. MICHAEL JETTER, 4. Physikalisches Institut, Universität Stuttgart, „*Wachstum und Dotierung von (In,Al,Ga)N*“
- 14.07. ELIF ARICI, LIOS, Universität Linz, „*Bulk heterojunction devices based on semiconducting polymers and inorganic core/shell nanomaterials*“
- 20.10. ALOIS KROST, Abteilung Halbleiterpitaxie, Universität Magdeburg, „*GaN-basierte Epitaxie und Bauelemente auf Silicium Substraten*“
- 27.10. ROLAND SCHEER, Bereich Solarenergie, Hahn-Meitner-Institut, Berlin, „*Defect ordering in CuB^{II}C^{VII}₂ ternary chalcogenides*“
- 10.11. HANSJÖRG GABLER, ZSW Stuttgart, „*Sonne und Wind für die Elektrifizierung netzferner Regionen in China*“
- 17.11. LUDWIG JÖRISSEN, ZSW Ulm, „*Brennstoffzellen – Stand der Technik und Perspektiven*“
- 24.11. ULF BLIESKE, Saint Gobain Glass, Herzogenrath, „*Textured glass for photovoltaic applications*“
- 1.12. MICHÈLE BOLTE, CNRS, Université Clermont-Ferrand, „*Primary process in dichromated photosensitive materials: interactivity Photochemistry – Holography*“
- 8.12. URSULA EICKER, Fachhochschule Stuttgart, „*Multifunktionalität der PV in PV-/Luftkollektor-Fassadensystemen für Wärmeproduktion u. thermische Kühlung*“
- 15.12. STEPHAN KLEINDIEK, Kleindiek Nanotechnik GmbH, Reutlingen, „*Nanotechnologie*“

10 Gäste und Stipendiaten 2003 / Guests 2003

AL TARABSHEH, ANAS, Jordan University of Science and Technology, Jordanien, 1.03.03 – 1.03.04

CARLSSON, ANNE, Uppsala Universitet, Schweden
01.03.02 – 31.07.03

CARLSSON, CAROLINE, Göteborgs Universitat, Schweden
1.03.03 – 31.12.04

DEKKER, TACO, Technical University of Delft, Holland
01.08.03 – 15.11.03

DENG, XUNMING, University of Toledo, Spanien
01.09.03 – 30.11.03

ESTURO BRETON, Ainhoa, UPV-Universidad del Pais Vasco, Spanien,
01.12.2001 – 30.09.2005

GARIN, MOISES, Universitat Politècnica de Catalunya, Barcelona, Spanien
01.03.03 – 31.08.03

IRUKULLA, ANAND KUMAR, Solar Energy Research Center – Borlänge, Schweden, 01.06.03 – 31.12.03

ISHIKAWA, YASUAKI, Nara Institute of Science and Technology, Japan
1.04.03 – 31.03.04

KAUK, MARIT, Tallin Technical University, Estland
6.10. – 31.12.03

LEESE, AARON, Pennsylvania State University, USA
01.09.03 – 31.12.03

NGUYEN, HONG QUANG, National Center for Natural Science and Technology, Hanoi, Vietnam, 1.10.1999 – 30.09.2004

NGUYEN, XUAN VIET, National Center for Natural Science and Technology,
Hanoi, Vietnam, 1.11.2001 – 30.09.2004

PAWLAK, WOJCIECH, Technical University of Lodz, Polen
01.08.03 – 15.10.03

POPADYNETS, YURIY, National Technical University of Ukraine, Kiev,
Ukraine, 1.03.03 – 31.08.03

TARETTO ZEYEN, KURT, Universidad Nacional del Comahue, Buenos Aires,
Argentinien, 01.01.1999 – 31.12.03

TURCU, MIRCEA, National Institute for Research and Development in
Electrochemistry and Condensed Matters, Timisoara, Rumänien,
1.04.1999 – 31.12.03

TOBAIL, OSAMA, Arab Academy for Science and Technology & Maritime
Transport, Alexandria, Ägypten, 01.07.03 – 30.06.04

YI, MAOXIANG, Hefei University of Technology, Baoding, China
01.10.02 – 31.08.03

ZHU, MINJI, Shanghai TEMIC Microsystems Co., China
15.04.03 – 15.04.04

11 Wissenschaftliche Geräte und Analysemethoden / Scientific Instruments and Methods of Analysis

11.1 Abscheideverfahren / Deposition Methods

Material / Materials	Abscheideverfahren / Deposition method	Anwendung / Application	Kontakt / Contact
Amorphe Halbleiter / <i>amorphous semiconductors</i> (a-Si:H, nc-Si, etc.)	Plasma-CVD (DC, RF, VHF), Niedertemperatur (70°C)/ <i>low temp. deposition</i> (70°C) thermokatalytische Depos. <i>hot-wire-CVD</i> Legierung / <i>alloying</i> (Ge, C) Dotierung / <i>doping</i> (B,P,...)	Dünnschicht- Solarzellen und Sensoren / <i>thin-film solar cells and sensors</i>	Schubert
Kristallines Silicium / <i>crystalline silicon</i> (mono, poly-Si)	CVD, RT-CVD, Plasma-CVD Hot-wire- CVD Ionenassistierte Epitaxie / <i>Ion Assisted Deposition (IAD)</i>	Dünnschicht- Solarzellen und Elektronik / <i>thin-film solar cells and electronics</i>	Schubert
Kristallines Silicium / <i>crystalline silicon</i>	Laserkristallisation / <i>laser crystallization</i>	Dünnschicht- transistoren / <i>thin-film transistors</i>	Köhler
Poröses Silicium / <i>porous silicon</i>	Transferverfahren / <i>transfer methods</i>	Elektronik auf Glas und flexiblen Sustraten / <i>Electronics on glass and flexible substrates</i>	Schubert
Polykristalline Verbindungs- halbleiter / <i>compound semiconductors</i> Cu(In,Ga)(Se,S) ₂ CdS, ZnS, ZnSe,	Aufdampfung, mit mehreren Quellen und individueller Ratenregelung, Katodenzerstäubung, chemische Badabscheidung / <i>multi- source evaporation, sputtering, chemical bath deposition</i>	Dünnschicht- Solarzellen / <i>thin-film solar cells</i>	Schock
Transparente leitfähige Schichten / <i>transparent conducting films</i> ITO, ZnO, SnO ₂	Katodenzerstäubung / <i>sputtering</i> (RF, DC, reactive)	Solarzellen und Sensoren / <i>solar cells and sensors</i>	Schock, Schubert

11.2 Strukturelle Analysenverfahren / Structural Materials Analysis

Methode / Method	Material / Materials	Anwendung / Application	Kontakt / Contact
Photoelektronenspektroskopie / <i>photoelectron spectroscopy</i> (small spot XPS/- ESCA, UPS)	Halbleiter Oberflächen, Dünnsschichten / <i>semiconductor surfaces,</i> <i>thin-films</i> CuInSe ₂ , ZnO	Solarzellen (in-situ Studien des Wachstums, elektronische Bandstruktur) / <i>solar</i> <i>cell materials (growth,</i> <i>band structure)</i>	Bilger
Sekundär-Ionen-Massenspektrometrie / <i>Secondary Ion Mass Spectroscopy</i> (SIMS)	Dünne Schichten, Schichtsysteme / <i>compositional analysis of</i> <i>thin films</i>	Laterale Elementverteilungen, Tiefenprofile, SpurenELEMENTE / <i>lateral element</i> <i>distribution, depth</i> <i>profiles, trace</i> <i>elements</i>	Bilger
Diffaktometrie (streifender Einfall) / <i>grazing incidence X-ray diffraction</i>	Silicium-, Verbindungshalbleiterschichten / <i>thin-film silicon and</i> <i>compound semiconductors</i>	Phasenanalyse, Textur von dünnen Schichten / <i>phase analysis, texture</i> <i>of thin films</i>	Schock
Rasterelektronenmikroskopie (incl. Röntgenanalyse) / <i>scanning electron microscopy, energy dispersive x-ray analysis</i>	Mikro- und polykristalline Dünnsschichten / <i>micro- and polycrystalline</i> <i>thin films</i>	Struktur, chemische Zusammensetzung, Tiefenprofile / <i>structure, chemical</i> <i>composition, depth</i> <i>profiling</i>	Schock

11.3 Analyse optischer Eigenschaften/ Analysis of Optical Properties

Methode / Method	Material	Anwendung / Application	Kontakt / Contact
FT-IR-Spektroskopie / <i>FT-IR-spectroscopy</i>	wasserstoffhaltige, amorphe und mikrokristalline Dünnschichthalbleiter / <i>hydrogen-containing amorphous and microcrystalline thin-film semiconductors</i>	Solarzellen, Sensoren (Wasserstoffgehalt, strukturelle Eigenschaften) / <i>solar cells, sensors</i>	Schubert
Raman-Spektroskopie / <i>Raman-spectroscopy</i>	amorphe und mikrokristalline dünne Schichten / <i>amorphous and microcrystalline thin films</i>	Solarzellen, Sensoren (strukturelle Eigenschaften) / <i>solar cells, sensors</i>	Schubert
Photolumineszenz / <i>photoluminescence</i>	Silizium, Verbindungs-halbleiter / <i>silicon, compound semiconductors</i>	Charakterisierung von Halbleitern / <i>characterization of semiconductors</i>	Rau
Photothermische Ablenkungs-Spektroskopie / <i>photothermal deflection spectroscopy</i> (PDS) Methode des konst. Photostroms./. <i>Constant photocurrent method</i> (CPM)	dünne Schichten / <i>thin films</i>	optische von Absorption Halbleiterschichten / <i>optical absorption of semiconductor thin films</i>	Schubert
Transmission, Reflexion / <i>optical transmission and reflection</i> (UV to NIR, direct, diffuse)	dünne Schichten für Solarzellen, Sensorik und Optoelektronik / <i>thin films for solar cells, sensors, and optoelectronics</i>	Bestimmung von Schichtdicke, Brechungsindex, Extinktionskoeffizient / <i>film thickness, refractive index, absorption</i>	Rau
In-situ Ellipsometrie / <i>in-situ ellipsometry</i>	dünne Schichten, Mehrschichtsysteme / <i>thin films, multi-layer systems</i>	Schichtwachstum und Grenzflächeneffekte / <i>film growth</i>	Schubert

11.4 Analyse elektro-optischer Eigenschaften / Analysis of Electro-Optical Properties

Methode / Method	Material / Materials	Anwendung / Application	Kontakt / Contact
Stationäre und transiente Photo- und Dunkel- leitfähigkeit / <i>stationary and transient dark- and photoconductance</i>	amorphe und polykristalline Dünnschichthalbleiter / <i>amorphous and polycrystalline thin-film semiconductors</i>	Bestimmung von Trägerdichten, Diffusionslängen, Fermi-Energie / <i>carrier densities, diffusion lengths, Fermi energy, etc.</i>	Schubert
Hall Messungen, Time-Of-Flight Spektroskopie, Quantenausbeute, transiente Mikrowellen- absorption / <i>Hall measurements, Time-Of-Flight (TOF) spectros- copy, quantum efficiency, μ-wave absorption</i>	Halbleitermaterialien und- bauelemente / <i>semiconductor materials and devices</i>	Trägerbeweglichkeiten, Rau Diffusionslängen, Minoritätsträger- lebensdauer, elektro- nische Zustandsdichte / <i>carrier mobilities, diffusion lengths, minority carrier lifetime, densities of states</i>	Rau
Admittanz- Spektroskopie, DLTS, modulierte Photoströme / <i>admittance, DLTS, modulated photocurrents</i>	Dünnschichthalbleiter und- bauelemente / <i>thin-film semiconductors and devices</i>	Solarzellen, Sensoren (Defekte, elektrische Transporteigenschaften interne Barrieren) / <i>solar cells, sensors (defects, electronic transport, internal barriers)</i>	Rau
IU-Kennlinien / <i>IV characteristics</i>	Dioden, Solarzellen / <i>diodes, solar cells</i>	Transporteigensch. / <i>transport properties</i>	Rau
Spektrale Empfindlichkeit, Quantenwirkungs- grad / <i>Spectral response Quantum- efficiency</i>	Dioden, Solarzellen / <i>diodes, solar cells</i>	Transporteigenschaften Rau optische Eigenschaften / <i>transport properties optical properties</i>	

12 Mitarbeiter / Staff Members

Name	Titel	Tel. 0711-685- ...	E-Mail ...@ipe.uni- stuttgart.de	Arbeitsgebiet
AL TARABSHEH, ANAS IBRAHIM	MSc	7179	al.tarabsheh	Optimierung und Charakterisierung von amorphen Silicium-Solarzellen
ALBERTS, LUKAS	Dr.-Ing.	7142	alberts	Abscheidungen von amorphen Silicium bei tiefen Temperaturen
BAUER, LEO		7182	bauer	Metallisierung, Photoarbeiten, Maskentechnik
BERGE, CHRISTOPHER	Dipl.-Phys.	7162	berge	Dünnschicht-Solarzellen aus kristallinem Silicium
BILGER, GERHARD	Dr.-Ing.	7176, 7154	bilger	Oberflächenanalytik mit SIMS und XPS; Technologie-Support
BRENDLE, WILLI	Dipl.-Ing.	7178	brendle	Niedertemperaturpassivierung für Transfer-Solarzellen
BRENNER, KLAUS	Dipl.-Ing. (FH)	7201	brenner	Technologische Infrastruktur und Prozesse der Si-Technologie
CARLSSON, CAROLINE		7160	carlsson	Hocheffiziente Solarzellen für Konzentratoren
DIEGEL, LYDIA		7163	diegel	Verwaltung
EISENMANN, LORENZ		7162	eisenmann	Dünnschichttechnik, Aufdampfverfahren
ESTURO-BRETON, AINHOA		7169	esturo-breton	Laserprozessierung von Silicium Solarzellen
GLÄSER, GERDA	Dipl.-Ing.	7168	glaeser	Charakterisierung von Monograin-Solarzellen
GRABITZ, PETER	Dipl.-Phys.	7197	grabitz	Flexible Verbindungshalbleiter-Solarzellen
HANNA, GEORGE	Dipl.-Phys.	7171	hanna	Hochleistungs-Cu(In,Ga)Se ₂ -Solarzellen, Abscheidung und Analyse von CIGS
HARDING, ADRIAN	M.A.	7196	harding	Photoelektronenspektroskopie, Röntgenbeugung
ISHIKAWA, YASUAKI	Dr.-Ing.	7167	ishikawa	Serienverschaltung von flexiblen a-Si Solarzellen
JACKSON, PHILIP	Dipl.-Phys.	7198	jackson	Flexible Substrate
KESSLER, ISABEL	M.A.	7141	kessler	Sekretariat, Verwaltung
KÖHLER, CHRISTIANE	Dipl.-Phys.	7182	ckoehler	Si-Niedertemperaturtechnologie, XRD, transparente Kontakte, Ramanstreuung
KÖHLER, JÜRGEN	Dr.-Ing.	7159	jkoehler	Laser Annealing, Verwaltung

Institut für Physikalische Elektronik / *Institute of Physical Electronics*

KÜHNLE, DENNIS		7200	kuehnle	Aufdampfen von Halbleiterschichten
LAPTEV, VIKTOR	Dr. rer.nat.	7197	laptev	Chemische Schichtabscheidung, Röntgenbeugungsmessungen
LOPEZ, LUIS	Dipl.-Ing.	7168	lopez	Information Technology Online und Self-Study-Online
LUTZ, BRIGITTE		7200	lutz	Analytik, Elektrochemie, GCMS
MATTHEIS, JULIAN	Dipl.-Ing.	7161	mattheis	Optische Eigenschaften von Solarzellen
NGUYEN HONG QUANG	M.Sc.	7171	quang	Oberflächenchemie von Cu(In,Ga)Se ₂ , Pufferschichten
NGUYEN XUAN VIET	M. Sc.	7179	viet	a.Si:H/c-Si Heterostrukturen
ORGASSA, KAY	Dipl.-Phys.	7181	orgassa	Optische Optimierung von CIGS-Solarzellen
PFISTERER, FRITZ	Dr.-Ing.	7157	pfisterer	Organisation / Verwaltung / allgemeine Aufgaben / Lehre (Optoelektronik I)
RAKHLIN, MICHAIL	Dipl.-Phys.	7183	rakhlin	Thermoelektrik, Silicium-Germanium-Dünnschichten
RAU, UWE	Dr. rer. nat.	7199	rau	Elektrische Charakterisierung und Modellierung von Dünnschichtsolarzellen (CIGS, Si, org.)
Riß, ANTON		7214	riss	Werkstatt
ROSTAN, JOHANNES	Dipl.-Ing.	7161	rostan	Dünnschichtsolarzellen
SCHLENKER, THOMAS	Dipl.-Phys.	7178	schlenker	Wachstum dünner CIGS Absorberschichten
SCHLÖTZER, THOMAS	Dipl.-Phys.	7181	schloetzer	In-situ Prozessierung von Dünnschichtsolarzellen
SCHOCK, HANS-WERNER	Dr.-Ing.	7180	schock	Dünnschichttechnik, Photovoltaik-Dünnschichtsolarzellen aus Verbindungshalbleitern
SCHUBERT, MARKUS	Dr.-Ing.	7145	schubert	Projektleitung amorphes und nanokristallines Si, Solarzellen mit Sensoren, Studien- und Diplomarbeiten, www.
STROHM, ANDREAS	Dr.rer.nat..	7142	strohm	Oberflächenanalytik und Cd-freie Pufferschichten für CIGS-Solarzellen
TARETTO-ZEYEN, KURT	Dipl.-Ing.	7181	tarett	Simulation und elektrische Charakterisierung von Halbleitern
TOBAIL, Osama	M. Sc.	7183	tobail	Verlustanalyse von CIGS-Solarzellen
TURCU, MIRCEA	M.Sc.	7184	turcu	Strukturelle und optische Eigenschaften von Cu(In,Ga)Se ₂

Jahresbericht 2003 / Annual Report 2003

V. REKOWSKI, CHRISTINE	Dr. phil.	7141	rekowski	Sekretariat, Verwaltung
WAGNER, MARTIN	Dipl.-Phys.	7184	martin.wagner	Dünnschichtprozesse
WERNER, JÜRGEN	Prof. Dr. rer. nat. habil.	7140	werner	Institutsleitung
WIESNER, HOLM	Dipl.-Ing.	7197	wiesner	CIS-Technologie
WILLE, WERNER		7158	wille	Buchhaltung, Verwaltung
ZHU, MINJI		7163	zhu	Optimierung von kristallinen Silicium-Solarzellen, QMS Transferschichten

13 Lageplan / Site Plan

